IEEE Access
Multidisciplinary : Rapid Review : Open Access Journal

Received August 12, 2020, accepted September 2, 2020, date of publication September 14, 2020,
date of current version September 25, 2020.

Digital Object Identifier 10.1109/ACCESS.2020.3023715

Finite-Time Synchronization of Multi-Linked Memristor-Based Neural Networks With Mixed Time-Varying Delays

SHAOFANG WANG[1,2], LIXIANG LI[1,2], HAIPENG PENG[1,2], YIXIAN YANG[2],
AND MINGWEN ZHENG[3]
[1]State Key Laboratory of Networking and Switching Technology, Information Security Center, Beijing University of Posts and Telecommunications, Beijing 100876, China
[2]National Engineering Laboratory for Disaster Backup and Recovery, Beijing University of Posts and Telecommunications, Beijing 100876, China
[3]School of Mathematics and Statistics, Shandong University of Technology, Zibo 255000, China

Corresponding author: Lixiang Li (lixiang@bupt.edu.cn)

This work was supported by the National Natural Science Foundation of China under Grant 61771071, Grant 61972051, Grant 61932005, and Grant 61702307.

ABSTRACT This paper mainly investigates the finite-time synchronization and stability issue of a class of master-slave multi-linked memristor-based neural networks (MMNNs) with mixed time-varying delays via different state-feedback controllers. Based on some synchronization analytical techniques and Lyapunov functional method, sufficient criteria are obtained to ensure that the master-slave MMNNs systems can realize finite-time synchronization under the Filippov-framework. Three different controllers are designed to synchronize the MMNNs systems, and the settling time of finite-time synchronization is estimated in advance. The correctness and the feasibility of the proposed synchronization criteria are confirmed by three simulation examples.

INDEX TERMS Finite-time synchronization, multi-linked memristor-based neural networks (MMNNs), adaptive controller, time-varying delays.

I. INTRODUCTION

The memristor, firstly postulated by Chua [1], is a nonlinear two-terminal electronic element indicating the relationship between flux-linkage and charge. The resistance of the memristor can be adjusted by the charge and magnetic flux. Compared with common resistor, memristor has two distinct advantages. Firstly, its resistance varies with the amount of current passing through, and remains unchanged until a reverse current is received. Secondly, one can calculate the amount of charge by measuring its resistance, thus it can act as memory resistor. Besides, the memristor exhibits switching state-dependent characteristic and has nonvolatile memory storage, and shares many similarities with synapses which form the brain neural networks. Hence, the memristor can easily achieve synaptic behavior and simulate the dynamic behavior of neuronal synapses.

The basic functions of biological brain, such as learning, memorizing and forgetting, mainly depend on the plasticity of synapses, especially the ability of changing the plasticity of synapses, which is highly correlated with the previous action potential history [2]. At the same time, memristor is a kind of nonlinear resistor with memory function, whose resistance value can be changed by controlling the change of current, this is very similar to synapses.

In 2008, the HP labs fabricated the first memristor [3], after that, the researchers began to reconstruct the traditional artificial neural networks by replacing resistors with memristors, forming variable connection weights, and got the memristor-based neural networks (MNNs) [4] which was more consistent with the biological brain neural networks. Hence, MNNs is an promising tool to simulate the biological brain neural networks. MNNs can adapt to new data and models more quickly and significantly improve the computing, parallel and adaptive ability of neural networks. Many scholars have devoted themselves to the study of dynamical behavior of MNNs, such as synchronization [5], stability and stabilization [6], [7], passivity [8]–[12], dispassvity [13], [14], etc. Up to now, many scholars have proposed many kinds of memristor-based neural networks

The associate editor coordinating the review of this manuscript and approving it for publication was Mou Chen.

models, such as reaction-diffusion memristor-based neural networks [5], [8], [12], [15], inertial memristor-based neural networks [9], [10], Hopfield memristor-based neural networks [7], Cohen-Grossberg memristor-based neural networks [16]–[18], fractional-order memristor-based neural networks [19]–[23], etc. Synchronization and stabilization are considered to be the most important dynamical behavior of MNNs. In general, the synchronization issue of MNNs can be transformed into the stabilization issue of MNNs. Many scholars have studied the synchronization of MNNs, and many excellent kinds of synchronization and stabilization have been proposed, such as lag synchronization [24]–[26], exponential synchronization [27]–[30], decay synchronization [31], [32], asymptotic synchronization [33], [34], finite-time synchronization [35]–[37], etc. And many significant and excellent results have been reported. For example, exponential synchronization of MNNs was investigated in [24], [27], [30], [38], [39], the synchronization of fractional-order MNNs has been studied in [19], [20], [22], [33], and the synchronization of memristor-based bidirectional associative memory neural networks was investigated in [39]–[41].

In order to shorten the convergence time of synchronization between master-slave MNNs systems, many effective synchronization methods have been introduced,such as pinning control, intermitent control, finite-time synchronous control. Finite-time synchronous control method was firstly introduced in 1961 [42], with which the convergence time can be calculated in advance. Therefore, it has advantages in various practical engineering applications. It is of significant importance to study the finite-time synchronization control of MNNs. There have been numerous investigations about finite-time synchronization of MNNs, such as, finite-time synchronization of fractional-order MNNs has been studied in [20], [43], finite-time synchronization of delayed MNNs has been investigated in [44]–[46], finite-time synchronization of bidirectional associative memory MNNs has been studied in [23], [43], [47], etc.

Meanwhile, as we all know, there exist time delays in various applications, owning to the hardware implementation exists in engineering applications and transmitter delays in biological neural networks, etc. Delay can affect system stability, therefore, it is of significant importance to study the MNNs involving various time delays. Multi-linked memristor-based neural networks (MMNNs) introduced in [48] can be regarded as a combination of several single-linked MNNs, with each edge having its own transmission delay. Therefore, MMNNs is more consistent with biological brain neural network and has a stronger ability in modeling various real-world applications compared with single-linked MNNs. Many scholars pay considerable attention to investigating the finte-time synchronization and stabilization of MNNs involving various time delays. And many excellent results have been reported, please see work [47], [49] and the references therein. However, there exist only few related literatures reporting the synchronization and stabilization control of MMNNs, please see [46], [48]. In [46], Qin *et al.* studied finite-time projective synchronization of multi-linked memristor-based neural network involving leakage delays. Therefore, the finite-time synchronzation issue on MMNNs is far from being fully studied, and there is little research on MMNNs with time-varying delays.

Motivated by the above discussions, this paper aims to investigate the finite-time synchronization problem of MMNNs involving both discrete time-varying delays and distributed time-varying delay by adopting different control strategies.

Our main contributions are:

(1) Three different controllers are designed. The first one is a linear and delay-independent state-feedback controller, the second one is a non-linear adaptive and delay-independent state-feedback controller, and the last one is a nonlinear and delay-dependent state-feedback controller. Our proof procedures adopted are simple to implement in practical applications.

(2) Three different Lyapunov-Krasovskii functionals are designed. Sufficient criteria are derived to ensure that the master-slave MMNNs systems can realize finite-time synchronization under the Filippov-Framework.

(3) The correctness and the feasibility of the acquired criteria are verified by three simulation examples.

Notation. For simplicity, the following symbols are to be adopted. $\mathbb{R}$, $\mathbb{R}^n$, $\mathbb{R}^{n_1\times n_2}$ represent the set of real number, n-dimensional Euclidean space, and a collection of matrices with dimension of $n_1\times n_2$, respectively. The sign of T denotes the transposition operation of a vector or matrix. $\mathbb{C}([-\tau,0],\mathbb{R}^n)$ represents a Banach space of continuous functions mapping the interval of $[-\tau,0]$ into $\mathbb{R}^n$. $\overline{co}[\check{\mathcal{W}},\hat{\mathcal{W}}]$ represents the closure of convex hull formed by the matrices or numbers $\check{\mathcal{W}}$ and $\hat{\mathcal{W}}$. For a matrix or vector $\mathbb{W}$, $\|\mathbb{W}\|_1$, $\|\mathbb{W}\|_\infty$, denote its $1-$norm, $\infty-$norm, respectively.

II. PRELIMINARIES AND MMNNs MODELS

A. DESCRIPTION OF MMNNs SYSTEMS

In this paper, we focus on studing the master-slave synchronization problem of multi-linked memristor-based neural networks (MMNNs) with mixed time-varying delays consisting of n nodes, and there exist m different links between any two nodes of the MMNNs systems. The master-slave MMNNs systems can be described by the following two differential equations.

The master MMNNs system is described as

$$\begin{aligned}\dot{z}_k(t) = &-\gamma_k z_k(t)+\sum_{s=1}^{n} w_{ks}(z_k(t))h_s(z_s(t))\\&+\sum_{s=1}^{n}\sum_{l=1}^{m} v_{(l)ks}(z_k(t))g_s(z_s(t-\tau_l(t)))\\&+\sum_{s=1}^{n} c_{ks}(z_k(t))\int_{t-\varrho(t)}^{t} f_s(z_s(x))dx+J_k(t),\\&t\geq 0, k=1,2,\ldots,n,\end{aligned}\tag{1}$$

The corresponding slave MMNNs system can be expressed as

$$\begin{aligned}\dot{y}_k(t) =& -\gamma_k y_k(t)+\sum_{s=1}^{n} w_{ks}(y_k(t))h_s(y_s(t))\\&+\sum_{s=1}^{n}\sum_{l=1}^{m} v_{(l)ks}(y_k(t))g_s(y_s(t-\tau_l(t)))\\&+\sum_{s=1}^{n} c_{ks}(y_k(t))\int_{t-\varrho(t)}^{t} f_s(y_s(x))dx+J_k(t)\\&+\mu_k(t), \quad t\geq 0,\ k=1,2,\ldots,n,\end{aligned} \tag{2}$$

where $z_k(t)$, $y_k(t)$ represent state variables of the kth neuron of the master-slave MMNNs systems (1) and (2), respectively; γ_k represents the rate of neuron self-inhibition; $h(\cdot)$, $g(\cdot)$ and $f(\cdot)$ stand for activation functions without and with time-varying delays; $\tau_l(t)$ denotes discrete time-varying delay, $l = 1,2,\ldots,m$, which satisfies $0 \leq \tau_l(t) \leq \tau$; $\varrho(t)$ represents distributed delay satisfying $0 \leq \varrho(t) \leq \varrho_M$; $\mu_i(t)$ is the controller to be determined later; $J_k(t)$ is the external input; $w_{ks}(\cdot)$, $v_{(l)ks}(\cdot)$, and $c_{ks}(\cdot)$ represent memristive connection weights which satisfy

$$\begin{aligned}w_{ks}(z_k(t)) &= \frac{\mathcal{M}_{ks}}{\mathcal{C}_k}\times sign_{ks},\\ v_{(l)ks}(z_k(t)) &= \frac{\mathcal{M}^{*}_{(l)ks}}{\mathcal{C}_k}\times sign_{ks},\\ c_{ks}(z_k(t)) &= \frac{\mathcal{M}^{**}_{ks}}{\mathcal{C}_k}\times sign_{ks},\quad sign_{ks}=\begin{cases}1, & k\neq s,\\ -1, & k=s,\end{cases}\end{aligned}$$

where $k = 1,2,\ldots,n$. Here, $\mathcal{C}_k$ denotes the value of the k-th capacitor, $\mathcal{M}_{ks}$, $\mathcal{M}^{*}_{(l)ks}$, $\mathcal{M}^{**}_{ks}$ denote the memductances of memristors $\mathcal{R}_{ks}$, $\mathcal{R}^{*}_{(l)ks}$, $\mathcal{R}^{**}_{ks}$, respectively. Moreover, $\mathcal{R}_{ks}$ represents the memristor between $h_s(z_s(t))$ and $z_k(t)$, or the memristor between $h_s(y_s(t))$ and $y_k(t)$, $\mathcal{R}^{*}_{(l)ks}$ represents the memristor between $g_s(z_s(t-\tau_l(t))$ and $z_k(t)$, or the memristor between $g_s(y_s(t-\tau_l(t))$ and $y_k(t)$, $\mathcal{R}^{**}_{ks}$ represents the memristor between $\int_{t-\varrho(t)}^{t} f_s\,(z_s(x))\,dx$ and $y_k(t)$, or the memristor between $\int_{t-\varrho(t)}^{t} f_s\,(y_s(x))\,dx$ and $z_k(t)$. $J_k(t)$ represents the external input. According to the characteristics of the memristors, we set the connection weights as follows:

$$w_{ks}(x_k(t)) = \begin{cases} w^{*}_{ks}, & |x_k(t)| \leq \mho_k,\\ invariant, & |x_k(t)| = \mho_k,\\ w^{**}_{ks}, & |x_k(t)| > \mho_k,\end{cases}$$

$$v_{(l)ks}(x_k(t)) = \begin{cases} v^{*}_{(l)ks}, & |x_k(t)| \leq \mho_k,\\ invariant, & |x_k(t)| = \mho_k,\\ v^{**}_{(l)ks}, & |x_k(t)| > \mho_k,\end{cases}$$

$$c_{ks}(x_k(t)) = \begin{cases} c^{*}_{ks}, & |x_k(t)| \leq \mho_k,\\ invariant, & |x_k(t)| = \mho_k,\\ c^{**}_{ks}, & |x_k(t)| > \mho_k,\end{cases}$$

where $k,s = 1,2,\ldots,n, l = 1,2,\ldots,m$, $x_k(t)$ represents $z_k(t)$ or $y_k(t)$, and $\mho_k$ is a positive constant, denoting the switching jumps thresholds. The invariant value means unchanged, w^{*}_{ks}, w^{**}_{ks}, $v^{*}_{(l)ks}$, $v^{**}_{(l)ks}$, c^{*}_{ks} and c^{**}_{ks} are known constants.

The initial values of MMNNs systems (1) and (2) are $\psi(s) = (\psi_1, \psi_2, \ldots, \psi_n(s))^T \in \mathbb{C}([-\tau,0],\mathbb{R}^n)$, and $\phi(s) = (\phi_1(s), \phi_2(s), \ldots, \phi_n(s))^T \in \mathbb{C}([-\tau,0],\mathbb{R}^n)$, respectively, where $\tau = \max\limits_{1\leq l\leq m}\{\tau_l(t), \varrho(t)\}$.

In order to simplify proof process, we make the following notation:

$$\begin{aligned}\hat{w}_{ij} &= \max\{w^{*}_{ij},\ w^{**}_{ij}\},\ \check{w}_{ij} = \min\{w^{*}_{ij}, w^{**}_{ij}\},\\ \tilde{w}_{ij} &= \max\{|w^{*}_{ij}|, |w^{**}_{ij}|\},\ \hat{v}_{(l)ij} = \max\{v^{*}_{(l)ij}, v^{**}_{(l)ij}\},\\ \check{v}_{(l)ij} &= \min\{v^{*}_{(l)ij}, v^{**}_{(l)ij}\},\ \tilde{v}_{(l)ij} = \max\{|v^{*}_{(l)ij}|, |v^{**}_{(l)ij}|\},\\ \hat{c}_{ij} &= \max\{c_{ij}, c^{**}_{ij}\},\ \check{c}_{ij} = \min\{c^{*}_{ij}, c^{**}_{ij}\},\\ \tilde{c}_{ij} &= \max\{|c^{*}_{ij}|, |c^{**}_{ij}|\}.\end{aligned}$$

We can write them in matrix forms, and get $\check{W} = (\check{w}_{ks})_{n\times n}$, $\check{V}_l = \left(\check{v}_{(l)ks}\right)_{n\times n}$, $\check{C} = (\check{c}_{ks})_{n\times n}$, $\hat{W} = \left(\hat{w}_{ks}\right)_{n\times n}$, $\hat{V}_l = \left(\hat{v}_{(l)ks}\right)_{n\times n}$, $\hat{C} = \left(\hat{c}_{ks}\right)_{n\times n}$, $\widetilde{W} = (\tilde{w}_{ks})_{n\times n}$, $\widetilde{V}_l = \left(\tilde{v}_{(l)ks}\right)_{n\times n}$, $\widetilde{C} = (\tilde{c}_{ks})_{n\times n}$.

According to the above descriptions, we can conclude that MMNNs systems (1) and (2) are switching systems with discontinuous right-hand side. Therefore, based on set-valued mapping and differential inclusions principle [50], the MMNNs systems (1) and (2) can be expressed in the following differential inclusions forms,

$$\begin{aligned}\dot{z}_k(t) \in& -\gamma_k z_k(t)+\sum_{s=1}^{n}\overline{co}\left[w_{ks}(z_k(t))\right]h_s(z_s(t))\\&+\sum_{s=1}^{n}\sum_{l=1}^{m}\overline{co}\left[v_{(l)ks}(z_k(t))\right]g_s(z_s(t-\tau_l(t)))\\&+\sum_{s=1}^{n}\overline{co}\left[c_{ks}(z_k(t))\right]\int_{t-\varrho(t)}^{t} f_s(z_s(x))dx+J_k(t),\end{aligned} \tag{3}$$

and

$$\begin{aligned}\dot{y}_k(t) \in& -\gamma_k y_k(t)+\sum_{s=1}^{n}\overline{co}\left[w_{ks}(y_k(t))\right]h_s(y_s(t))\\&+\sum_{s=1}^{n}\sum_{l=1}^{m}\overline{co}\left[v_{(l)ks}(y_k(t))\right]g_s(y_s(t-\tau_l(t)))\\&+\sum_{s=1}^{n}\overline{co}\left[c_{ks}(y_k(t))\right]\int_{t-\varrho(t)}^{t} f_s(y_s(x))dx+\mu(t)+J_k(t),\end{aligned} \tag{4}$$

for $k = 1,2,\ldots,n,$, and $\overline{co}[w_{ij}(\cdot)]$, $\overline{co}[v_{(l)ij}(\cdot)]$, $\overline{co}[c_{ij}(\cdot)]$ are the closure of convex hull generated by the sets $[w_{ij}(\cdot)]$, $[v_{(l)ij}(\cdot)]$, $[c_{ij}(\cdot)]$, respectively. Their values are given by

$$\overline{co}[w_{ks}(x_i(t))] = \begin{cases} w^{*}_{ks}, & |x_k(t)| \leq \mho_k,\\ [\check{w}_{ij}, \hat{w}_{ij}], & |x_k(t)| = \mho_k,\\ w^{**}_{ks}, & |x_k(t)| > \mho_k,\end{cases}$$

$$\overline{co}[v_{(l)ks}(x_k(t))] = \begin{cases} v^{*}_{(l)ks}, & |x_k(t)| \leq \mho_k,\\ [\check{v}_{(l)ks}, \hat{v}_{(l)ks}], & |x_k(t)| = \mho_k,\\ v^{**}_{(l)ks}, & |x_k(t)| > \mho_k,\end{cases}$$

$$\overline{co}[c_{ks}(x_k(t))] = \begin{cases} c_{ks}^{*}, & |x_k(t)| \le \mho_k, \\ [\breve{c}_{ks}, \hat{c}_{ks}], & |x_k(t)| = \mho_k, \\ c_{ks}^{**}, & |x_k(t)| > \mho_k, \end{cases}$$

here $x_k(t)$ represents $z_k(t)$ or $y_k(t)$.

Hence, there exist measurable functions $\acute{w}_{ks}(t) \in \overline{co}[w_{ks}(z_k(t))]$, $\acute{v}_{(l)ks}(t) \in \overline{co}[v_{(l)ks}(z_k(t))]$, $\acute{c}_{ks}(t) \in \overline{co}[c_{ks}(z_k(t))]$, $\grave{w}_{ks}(t) \in \overline{co}\left[\breve{w}_{ks}, \hat{w}_{ks}\right]$, $\grave{v}_{(l)ks}(t) \in \overline{co}\left[\breve{v}_{(l)ks}, \hat{v}_{(l)ks}\right]$ and $\grave{c}_{ks}(t) \in \overline{co}\left[\breve{c}_{ks}, \hat{c}_{ks}\right]$, such that

$$\begin{aligned} \dot{z}_k(t) = &-\gamma_k z_k(t) + \sum_{s=1}^{n} \acute{w}_{ks}(t) h_s(z_s(t)) \\ &+ \sum_{s=1}^{n}\sum_{l=1}^{m} \acute{v}_{(l)ks}(t) g_s(z_s(t-\tau_l(t))) \\ &+ \sum_{s=1}^{n} \acute{c}_{ks}(t) \int_{t-\varrho(t)}^{t} f_s(z_s(x))dx + J_k(t),\ t \ge 0. \end{aligned} \tag{5}$$

And

$$\begin{aligned} \dot{y}_k(t) = &-\gamma_k y_k(t) + \sum_{s=1}^{n} \grave{w}_{ks}(t) h_s(y_s(t)) \\ &+ \sum_{s=1}^{n}\sum_{l=1}^{m} \grave{v}_{(l)ks}(t) g_s(y_s(t-\tau_l(t))) \\ &+ \sum_{s=1}^{n} \grave{c}_{ks}(t) \int_{t-\varrho(t)}^{t} f_s(y_s(x))dx + \mu_k(t) + J_k(t), \end{aligned} \tag{6}$$

for $k = 1, 2, \ldots, n$.

The synchronization issue between MMNNs systems (1) and (2) can be transformed into the corresponding stability problem, the error system between MMNNs systems (1) and (2) is defined as $e_k(t) = y_k(t) - z_k(t)$, then we can get

$$\begin{aligned} \dot{e}_k(t) = \dot{y}_k(t) - \dot{z}_k(t) = &-\gamma_k e_k(t) \\ &+ \sum_{s=1}^{n} (\grave{w}_{ks}(t) - \acute{w}_{ks}(t)) h_s(y_s(t)) + \sum_{s=1}^{n} \acute{w}_{ks}(t) H_s(e_s(t)) \\ &+ \sum_{s=1}^{n}\sum_{l=1}^{m} (\grave{v}_{(l)ks}(t) - \acute{v}_{(l)ks}(t)) g_s(y_s(t-\tau_l(t))) \\ &+ \sum_{s=1}^{n}\sum_{l=1}^{m} \acute{v}_{(l)ks}(t) G_s(e_s(t-\tau_l(t))) \\ &+ \sum_{s=1}^{n} (\grave{c}_{ks}(t) - \acute{c}_{ks}(t)) \int_{t-\varrho(t)}^{t} f_s(y_s(x))dx \\ &+ \sum_{s=1}^{n} \acute{c}_{ks}(t) \int_{t-\varrho(t)}^{t} F_s(e_s(x))dx + \mu_k(t),\ t \ge 0, \end{aligned} \tag{7}$$

for $k = 1, 2, \ldots, n$.

Or,

$$\begin{aligned} \dot{e}(t) = \dot{y}(t) - \dot{z}(t) = &-\Gamma e(t) + (\grave{W}(t) - \acute{W}(t)) h(y(t)) \\ &+ \acute{W}(t) H(e(t)) + \sum_{l=1}^{m} (\grave{V}_l(t) - \acute{V}_l(t)) g(y(t-\tau_l(t))) \\ &+ \sum_{l=1}^{m} \acute{V}_l(t) G(e(t-\tau_l(t))) \\ &+ (\grave{C}(t) - \acute{C}(t)) \int_{t-\varrho(t)}^{t} f(y(x))dx \\ &+ \acute{C}(t) \int_{t-\varrho(t}^{t} F(e(x))dx + \mu(t),\ t \ge 0, \end{aligned} \tag{8}$$

where $e(t) = (e_1(t), e_2(t), \ldots, e_n(t))^T$, $H(e(t)) = h(y(t)) - h(z(t))$, $F(e(t)) = f(y(t)) - f(z(t))$, $G(e(t-\tau_l(t))) = g(y(t-\tau_l(t))) - g(z(t-\tau_l(t)))$; And $\acute{W}(t) = (\acute{w}_{ks}(t))_{n\times n}$, $\grave{W}(t) = (\grave{w}_{ks}(t))_{n\times n}$, $\acute{V}_l(t) = (\acute{v}_{(l)ks}(t))_{n\times n}$, $\grave{V}_l(t) = (\grave{v}_{(l)ks}(t))_{n\times n}$, $\acute{C}(t) = (\acute{c}_{ks}(t))_{n\times n}$, $\grave{C}(t) = (\grave{c}_{ks}(t))_{n\times n}$. Besides, the error system (8) takes the initial value $\varphi(s) = \psi(s) - \phi(s) \in \mathbb{C}([-\tau, 0], \mathbb{R}^n)$.

The results of this paper are based on one definition, two important lemmas and three assumptions, as follows:

Assumption 1: The functions $h(u)$, $g(u)$ and $f(u)$ are assumed to be bounded. Then for any $u \in \mathbb{R}^n$, there always exist positive constants ξ_k^h, ξ_k^g and ξ_k^f, for $k = 1, 2, \ldots, n$, which satisfy $|h_k(u_k)| \le \xi_k^h$, $|g_k(u_k)| \le \xi_k^g$, and $|f(u_k)| \le \xi_k^f$. We denote $\xi^h = \max_{1\le k\le n}\{\xi_k^h\}$, $\xi^g = \max_{1\le k\le n}\{\xi_k^g\}$, $\xi^f = \max_{1\le k\le n}\{\xi_k^f\}$, $\Xi^h = (\xi_1^h, \xi_2^h, \ldots, \xi_n^h)^T \in \mathbb{R}^n$, $\Xi^g = (\xi_1^g, \xi_2^g, \ldots, \xi_n^g)^T \in \mathbb{R}^n$ and $\Xi^f = \left(\xi_1^f, \xi_2^f, \ldots, \xi_n^f\right)^T \in \mathbb{R}^n$.

Assumption 2: The functions $h(x)$, $g(x)$ and $f(x)$ are assumed to be Lipschitz continuous in $x \in \mathbb{R}^n$. Then for any $u_k, v_k \in \mathbb{R}^n$, there exist positive constants ι_k^h, ι_k^g and ι_k^f, such that $|h_k(u_k) - h_k(v_k)| \le \iota_k^h|u_k - v_k|$, $|g_k(u_k) - g_k(v_k)| \le \iota_k^g|u_k - v_k|$, and $|f_k(u_k) - f_k(v_k)| \le \iota_k^h|u_k - v_k|$, where $1 \le k \le n$. And we denote that $L^h = \max_{1\le k\le n}\{\iota_k^h\}$, $L^g = \max_{1\le k\le n}\{\iota_k^g\}$, and $L^f = \max_{1\le k\le n}\left\{\iota_k^f\right\}$.

Assumption 3: $\varrho(t)$ and $\tau_l(t)$, $l = 1, 2, \ldots, m$ are continuously differential functions, which satisfy $0 \le \dot{\varrho}(t) \le \varrho_D < 1$, $0 \le \dot{\tau}_l(t) \le \tau_D < 1$. Here ϱ_D, τ_D are two known positive constants.

Lemma 1 [51]: If $\mathbb{V}(t)$ is a continuous function, and takes values between 0 and ∞, and satisfies

$$\dot{\mathbb{V}}(t) \le -\rho \mathbb{V}^{\varsigma}(t),\ \forall t \ge t_0, \quad \mathbb{V}(t_0) \ge 0,$$

where $\rho > 0$, $0 < \varsigma < 1$ are positive canstants. Then we can get

$$\mathbb{V}^{1-\varsigma}(t) \le \mathbb{V}^{1-\varsigma}(t_0) - \rho(1-\varsigma)(t - t_0),\ t_0 \le t \le t^*,$$

and $\mathbb{V}(t) \equiv 0$, $\forall t \ge t^*$, where t^* can be calculated by

$$t^* = t_0 + \frac{\mathbb{V}^{1-\varsigma}(t_0)}{\rho(1-\varsigma)}.$$

Lemma 2 [52]: Let $\nu_1, \nu_2, \ldots, \nu_n \ge 0$, where n is a postive integer, and $0 < \varepsilon \le 1$, then we conclude:

$$\sum_{\iota=1}^{n} \nu_\iota^{\varepsilon} \ge \left(\sum_{\iota=1}^{n} \nu_\iota\right)^{\varepsilon}.$$

Definition 1: The MMNNs (2) is regarded to be synchronized with the MMNNs (1) in finite time, if under certain appropriately designed controller(s), there exists a constant $t^* > 0$, such that $\lim_{t\to t^*} e(t) = (0, 0, \ldots, 0)^T$, and when $t \geq t^*$, $e(t) \equiv (0, 0, \ldots, 0)^T$ always holds, and t^* is called the settling time.

III. MAIN RESULTS

In this paper, three different controllers are designed in this section to realize finite-time synchronization between the MMNNs systems (1) and (2). Meanwhile, based on some synchronization analytical techniques, sufficient criteria are derived to ensure that the synchronization can be acquired in finite time.

A. LINEAR AND DELAY-INDEPENDENT STATE-FEEDBACK CONTROLLER

We adopt the following linear and delay-independent state-feedback controller

$$\mu(t) = -\varpi e(t) - \zeta\, sign(e(t)), \tag{9}$$

where $\varpi = (\varpi_1, \varpi_2, \ldots, \varpi_n)$, $\zeta = (\zeta_1, \zeta_2, \ldots, \zeta_n)$ are two vectors to be determined later. And

$$sign(e(t)) = (sign(e_1(t)), sign(e_2(t)), \ldots, sign(e_n(t)))^T$$

$\varpi_k > 0$, $\zeta_k > 0$, for $k = 1, 2, \ldots, n$.

Theorem 1: Assuming that Assumptions 1-3 hold, and we denote $\underline{\varpi} = \min_{1\leq k\leq n} \{\varpi_k\}$, and $\underline{\zeta} = \min_{1\leq k\leq n} \{\zeta_k\}$. if $\underline{\varpi}$, $\underline{\zeta}$ satisfy the following conditions:

$$\underline{\varpi} \geq \Big(-\underline{\gamma} + L^h \|\widetilde{W}\|_1 + \varrho_M L^f \|\widetilde{C}\|_1 + \frac{L^g}{1-\tau_D} \sum_{l=1}^{m} \|\widetilde{V}_l\|_1\Big),$$
$$\underline{\zeta} > \Big(\xi^h \|\hat{W} - \check{W}\|_\infty + \xi^g \Big(\sum_{l=1}^{m} \|\hat{V}_l - \check{V}_l\|_\infty\Big) + \varrho_M \xi^f \|\hat{C} - \check{C}\|_\infty\Big),$$

where $\underline{\gamma} = \min_{1\leq k\leq n} \{\gamma_k\}$. Then, after applying the controller (9) to the MMNNs system (2), the MMNNs systems (2) and (1) can achieve synchronization in finite time t_1^*, given by

$$t_1^* = \frac{\mathbb{V}(0)}{\Omega}, \tag{10}$$

where $\Omega = \underline{\zeta} - \xi^h \|\hat{W} - \check{W}\|_\infty - \xi^g \left(\sum_{l=1}^{m} \|\hat{V}_l - \check{V}_l\|_\infty\right) - \varrho_M \xi^f \|\hat{C} - \check{C}\|_\infty > 0$.

Proof: By utilizing the Generalized Lyapunov Construction method, we adopt the Lyapunov functional as follows:

$$\mathbb{V}(t) = \mathbb{V}_1(t) + \mathbb{V}_2(t) + \mathbb{V}_3(t), \tag{11}$$

where

$$\mathbb{V}_1(t) = \|e(t)\|_1,$$
$$\mathbb{V}_2(t) = \frac{L^g}{1-\tau_D} \sum_{l=1}^{m} \|\widetilde{V}_l\|_1 \int_{t-\tau_l(t)}^{t} \|e(x)\|_1 dx,$$
$$\mathbb{V}_3(t) = L^f \|\widetilde{C}\|_1 \int_{-\varrho_M}^{0} \int_{t+\vartheta}^{t} \|e(x)\|_1 dx d\vartheta. \tag{12}$$

Based on Chain rule introduced in [53], we can conclude that $\mathbb{V}(t)$ is a C-regular function, we can calculate the the derivatives of the functions $\mathbb{V}_1(t)$, $\mathbb{V}_2(t)$ and $\mathbb{V}_3(t)$, respectively.

Calculating the derivative of $\mathbb{V}_1(t)$ along the trajectory of (8) leads to

$$\dot{\mathbb{V}}_1(t) = sign^T(e(t))\Big[-\Gamma(t) + (\grave{W}(t) - \acute{W}(t))h(y(t)) + \acute{W}(t)H(e(t)) + \sum_{l=1}^{m} (\grave{V}_l(t) - \acute{V}_l(t))g(y(t-\tau_l(t))) + \sum_{l=1}^{m} \acute{V}_l(t)G(t-\tau_l(t)) + (\grave{C}(t) - \acute{C}(t)) \int_{t-\varrho(t)}^{t} f(y(x))dx + \acute{C}(t) \int_{t-\varrho(t}^{t} F(e(x))dx - \mu(t)\Big]. \tag{13}$$

Obviously,

$$sign^T(e(t))\,(-\Gamma(t)) = -\sum_{k=1}^{n} sign(e_k(t))(-\gamma_k e_k(t)) = -\sum_{k=1}^{n} \gamma_k |e_k(t)| \leq -\underline{\gamma}\|e(t)\|_1. \tag{14}$$

From Assumption 2, we can conclude that

$$sign^T(e(t))\acute{W}(t)H(e(t)) = \sum_{k=1}^{n}\sum_{s=1}^{n} sign(e_k(t))\acute{w}_{ks}(t)H_s((e_s(t))) \leq \sum_{k=1}^{n}\sum_{s=1}^{n} |\acute{w}_{ks}(t)| \iota_k^h |e_s(t)| \leq L^h \sum_{k=1}^{n}\sum_{s=1}^{n} |\acute{w}_{ks}(t)||e_s(t)| \leq L^h \|\widetilde{W}\|_1 \|e(t)\|_1, \tag{15}$$

Similarly, we can conclude

$$sign^T(e(t)) \sum_{l=1}^{m} \acute{V}_l(t)G(e(t-\tau_l(t))) \leq L^g \sum_{l=1}^{m} \|\widetilde{V}_l\|_1 \|e(t-\tau_l(t))\|_1, \tag{16}$$

and

$$sign^T(e(t))\acute{C}(t) \int_{t-\varrho(t)}^{t} F(e(x))dx \leq L^f \|\widetilde{C}\|_1 \int_{t-\varrho(t)}^{t} \|e(s)\|_1 ds \leq L^f \|\widetilde{C}\|_1 \int_{t-\varrho(t)}^{t} \|e(s)\|_1 ds. \tag{17}$$

Based on Assumption 1, we can obtain

$$sign^T(e(t))(\grave{W}(t) - \acute{W}(t))h(y(t)) = \sum_{k=1}^{n}\sum_{s=1}^{n} sign(e_k(t))(\grave{w}_{ks}(t) - \acute{w}_{ks}(t))h_s(y_s(t))$$

$$\le \sum_{k=1}^{n}\sum_{s=1}^{n}|\grave{w}_{ks}(t)-\acute{w}_{ks}(t)||sign(e_k(t))|\xi_s^h$$
$$\le \xi^h\|\hat{W}-\check{W}\|_\infty\sum_{k=1}^{n}\chi_k, \tag{18}$$

Similar to (18), we conclude that

$$sign^T(e(t))\sum_{l=1}^{m}(\grave{V}_l(t)-\acute{V}_l(t))g(y(t-\tau_l(t)))$$
$$=\sum_{k=1}^{n}\sum_{s=1}^{n}\sum_{l=1}^{m}sign(e_k(t))(\grave{v}_{(l)ks}(t)-\acute{v}_{(l)ks}(t))\cdot g_s(y_s(t-\tau_l(t)))$$
$$\le \sum_{k=1}^{n}\sum_{s=1}^{n}\sum_{l=1}^{m}|\hat{v}_{(l)ks}-\check{v}_{(l)ks}|\xi_s^g|sign(e_k(t))|$$
$$\le \sum_{k=1}^{n}\sum_{s=1}^{n}\sum_{l=1}^{m}|\hat{v}_{(l)ks}-\check{v}_{(l)ks}|\xi_s^g\chi_k$$
$$\le \xi^g\left(\sum_{l=1}^{m}\|\hat{V}_l-\check{V}_l\|_\infty\right)\sum_{k=1}^{n}\chi_k, \tag{19}$$

Similarly,

$$sign^T(e(t))(\grave{C}(t)-\acute{C}(t)\int_{t-\varrho(t)}^{t}f(y(x))dx$$
$$=\sum_{k=1}^{n}\sum_{s=1}^{n}sign(e_k(t))(\grave{c}_{ks}(t)-\acute{c}_{ks}(t))\cdot\int_{t-\varrho(t)}^{t}f(y(x))ds$$
$$\le \sum_{k=1}^{n}\sum_{s=1}^{n}|\hat{c}_{ks}-\check{c}_{ks}||sign(e_k(t))|\int_{t-\varrho(t)}^{t}\xi_s^f ds$$
$$\le \sum_{k=1}^{n}\sum_{s=1}^{n}(\hat{c}_{ks}-\check{c}_{ks})\chi_k\int_{t-\varrho_M}^{t}\xi_s^f ds$$
$$\le \varrho_M\xi^f\|\hat{C}-\check{C}\|_\infty\sum_{k=1}^{n}\chi_k. \tag{20}$$

On the other hand, we have

$$sign^T(e(t))\mu(t)$$
$$=\sum_{k=1}^{n}sign(e_k(t))(-\varpi_k e_k(t)-\zeta_k sign(e_k(t)))$$
$$=\sum_{k=1}^{n}\left(-\varpi_k|e_k(t)|-\zeta_k|sign(e_k(t))|^2\right)$$
$$\le -\underline{\varpi}\|e(t)\|_1-\underline{\zeta}\sum_{k=1}^{n}\chi_k, \tag{21}$$

where we define

$$\chi_k=((sign e_k(t)))^2=\begin{cases}0, & when\ e_k(t)=0,\\ 1, & else,\end{cases}$$

which means that $\chi_k=0$ if $e_k(t)=0$, otherwise $\chi_k=1$.

Then we can get

$$\dot{\mathbb{V}}_1(t)\le-\underline{\gamma}\|e(t)\|_1+\xi^h\|\hat{W}-\check{W}\|_\infty\sum_{k=1}^{n}\chi_k$$
$$+L^h\|\widetilde{W}\|_1\|e(t)\|_1+\xi^g\left(\sum_{l=1}^{m}\|\hat{V}_l-\check{V}_l\|_\infty\right)\sum_{k=1}^{n}\chi_k$$
$$+L^g\sum_{l=1}^{m}\|\widetilde{V}_l\|_1\|e(t-\tau_l(t))\|_1$$
$$+\varrho_M\xi^f\|\hat{C}-\check{C}\|_\infty\sum_{k=1}^{n}\chi_k+L^f\|\widetilde{C}\|_1\int_{t-\varrho(t)}^{t}\|e(s)\|_1ds$$
$$-\underline{\varpi}\|e(t)\|_1-\underline{\zeta}\sum_{k=1}^{n}\chi_k$$
$$=\left(-\underline{\gamma}+L^h\|\widetilde{W}\|_1-\underline{\varpi}\right)\|e(t)\|_1$$
$$+L^g\sum_{l=1}^{m}\|\widetilde{V}_l\|_1\|e(t-\tau_l(t))\|_1+\Big(\xi^h\|\hat{W}-\check{W}\|_\infty$$
$$+\xi^g\left(\sum_{l=1}^{m}\|\hat{V}_l-\check{V}_l\|_\infty\right)+\varrho_M\xi^f\|\hat{C}-\check{C}\|_\infty-\underline{\zeta}\Big)\sum_{k=1}^{n}\chi_k$$
$$+L^f\|\widetilde{C}\|_1\int_{t-\varrho_M}^{t}\|e(s)\|_1ds. \tag{22}$$

According to Assumptions 2 and 3, we can calculate the derivatives of $\mathbb{V}_2(t)$ and $\mathbb{V}_3(t)$, and obtain

$$\dot{\mathbb{V}}_2(t)=\frac{L^g}{1-\tau_D}\sum_{l=1}^{m}\Big(\|\widetilde{V}_l\|_1\|e(t)\|_1-\|\widetilde{V}_l\|_1\|e(t-\tau_l(t))\|_1(1-\dot{\tau}_l(t))\Big)$$
$$\le\frac{L^g}{1-\tau_D}\sum_{l=1}^{m}\left(\|\widetilde{V}_l\|_1\|e(t)\|_1\right)-L^g\sum_{l=1}^{m}\left(\|\widetilde{V}_l\|_1\|e(t-\tau_l(t))\|_1\right), \tag{23}$$

and

$$\dot{\mathbb{V}}_3(t)=L^f\|\widetilde{C}\|_1\int_{-\varrho_M}^{0}\|e(t)\|_1ds-L^f\|\widetilde{C}\|_1\int_{-\varrho_M}^{0}\|e(t+s)\|_1ds$$
$$\le\varrho_M L^f\|\widetilde{C}\|_1\|e(t)\|_1-L^f\|\widetilde{C}\|_1\int_{t-\varrho_M}^{t}\|e(s)\|_1ds. \tag{24}$$

Therefore, according to (22), (23), and (24), we can get that

$$\dot{\mathbb{V}}(t)=\dot{\mathbb{V}}_1(t)+\dot{\mathbb{V}}_2(t)+\dot{\mathbb{V}}_3(t)\le\Big(-\underline{\gamma}+L^h\|\widetilde{W}\|_1$$
$$+\varrho_M L^f\|\widetilde{C}\|_1+\frac{L^g}{1-\tau_D}\sum_{l=1}^{m}\|\widetilde{V}_l\|_1-\underline{\varpi}\Big)\|e(t)\|_1$$
$$+\Big(\xi^h\|\hat{W}-\check{W}\|_\infty+\xi^g\left(\sum_{l=1}^{m}\|\hat{V}_l-\check{V}_l\|_\infty\right)$$
$$+\varrho_M\xi^f\|\hat{C}-\check{C}\|_\infty-\underline{\zeta}\Big)\sum_{k=1}^{n}\chi_k. \tag{25}$$

We can easily conclude that

$$\dot{\mathbb{V}}(t) \leq -\hbar\|e(t)\|_1 - \Omega\sum_{k=1}^{n}\chi_k, \tag{26}$$

where

$$\hbar = -\Big[-\underline{\gamma} + L^h\|\widetilde{W}\|_1 + \varrho_M L^f\|\widetilde{C}\|_1 + \frac{L^g}{1-\tau_D}\sum_{l=1}^{m}\|\widetilde{V}_l\|_1 - \underline{\varpi}\Big].$$

According to Theorem 1, it concludes that

$$\dot{\mathbb{V}}(t) \leq -\hbar\|e(t)\|_1 - \Omega\sum_{k=1}^{n}\chi_k \leq -\Omega\sum_{k=1}^{n}\chi_k. \tag{27}$$

There are mainly two cases concerning the value of $\sum_{k=1}^{n}\chi_k$.

Case 1: Only when $e(t) \equiv 0$, which means that $e_k(t) = 0, k = 1, 2, \ldots, n$, we can get $\sum_{k=1}^{n}\chi_k = 0$. According to Definition 2.3, we can conclude that the MMNNs (2) is synchronized with the MMNNs (1).

Case 2: if $e(t) \neq 0$, which means that there exists at least one item $e^*(t)$ satisfying $e^*(t) \neq 0$, then we conclude that $\sum_{k=1}^{n}\chi_k \geq 1$. We can conclude from (29) that

$$\dot{\mathbb{V}}(t) \leq -\Omega\sum_{k=1}^{n}\chi_k \leq -\Omega < 0, \tag{28}$$

In this case, taking integral operation on both sides of the inequality (28) between regions (0, t), where $t > 0$, we further conclude that

$$\mathbb{V}(t) \leq \mathbb{V}(0) - \Omega t. \tag{29}$$

The inequality $\mathbb{V}(t) \geq 0$ always holds according to the definition of $\mathbb{V}(t)$. Since $\dot{\mathbb{V}}(t) < 0$, it can be concluded that when $t = t_1^* \geq \frac{\mathbb{V}(0)}{\Omega}$, $\mathbb{V}(t) \equiv 0$, which means $e_k(t) \equiv 0$, thus $\chi_k = (sign(e_k(t)))^2 \equiv 0$. Therefore, we can infer that $\sum_{k=1}^{n}\chi_k \equiv 0$. Further, we obtain

$$|e(t^*)|_1 = 0 \quad and \quad \|e(t)\|_1 \equiv 0,\ \forall t \geq t_1^*,$$

where $t_1^* = \frac{\mathbb{V}(0)}{\Omega}$.

According to Definition 1, we can conclude that the slave MMNNs system (2) can synchronize with the master MMNNs system (1) under the controller (9) during the settling time, given by $t_1^* = \frac{\mathbb{V}(0)}{\Omega}$.

The proof of Theorem 1 is finished.

Corollary 1: For master-slave MMNNs systems (1) and (2), if there exists only one link between any two nodes of the systems, which means $m = 1$, the MMNNs systems degenerate into single-linked MNNs systems. Under this condition, if $\underline{\varpi}$ and $\underline{\zeta}$ meet the following requirements:

$$\underline{\varpi} \geq -\underline{\gamma} + L^h\|\widetilde{W}\|_1 + \frac{L^g}{1-\tau_D}\|\widetilde{V}_1\|_1 + \varrho_M L^f\|\widetilde{C}\|_1,$$
$$\underline{\zeta} > \xi^h\|\hat{W} - \check{W}\|_\infty + \xi^g\|\hat{V}_1 - \check{V}_1\|_\infty + \varrho_M\xi^f\|\hat{C} - \check{C}\|_\infty.$$

then MNNs systems (1) and (2) with $m = 1$ can gain finte-time synchronization within a calculated time, which can be calculated in advance by utilizing (10) with $m = 1$.

Proof: The proof process is similar to that of Theorem 1, hence, we omit the proof process.

Remark 1: Corollary 1 can be viewed as a simple case of Theorem 1 since there is only one link between any two nodes of the MMNNs systems, or, in other words, they are MNNs systems which have been studied in [49], [54]. The exponential synchronization of delayed MNNs was investigated in [24].

B. NON-LINEAR ADAPTIVE AND DELAY-INDEPENDENT STATE-FEEDBACK CONTROLLER

In this subsection, we design an adaptive and non-linear state-feedback controller to realize the finite-time synchronization between MMNNs systems (1) and (2), the following controller is utilized

$$u_k(t) = -\varpi_k^*(t)e_k(t) - \zeta_k^*(t)sign(e_k(t)), \tag{30}$$

for $k = 1, 2, \ldots, n$, $\varpi_k^*(t), \zeta_k^*(t)$ are time-varying parameters. The adaptive laws of $\varpi_k^*(t), \zeta_k^*(t)$ are designed as follows:

$$\dot{\varpi}_k^*(t) = \varpi_k^*|e_k(t)|,$$
$$\dot{\zeta}_k^*(t) = \zeta_k^*|sign(e_k(t))|,$$

where ϖ_k^*, ζ_k^*, for $k = 1, 2, \ldots, n$ are unknown positive constants to be determined later.

Remark 2: The controller (30) also appears in Ref. [18], [37], [45], etc. Compared with the regular feedback controller (i.e. $\mu(t) = -ke(t)$), the controller (30) has two adaptive control parameters and is more flexible to use. We can also find a similar form of controller (30) in Refs. [15], [34], [41], [55], etc. However, these research results either deal with asymptotic control, or deal with different networks models. In comparison, the model in this paper is more general. In addition, adaptive control can modify its own characteristics to adapt to the dynamic characteristics of objects. Therefore, here we choose adaptive control.

Theorem 2. Based on Assumptions 1, 2, and 3, and if the control gains ϖ_k^*, ζ_k^* meet the following conditions

$$\varpi_k^* \geq \sum_{s=1}^{n}L^h\tilde{w}_{sk} + L^g\sum_{s=1}^{n}\sum_{l=1}^{m}\frac{\tilde{v}_{(l)sk}}{1-\tau_D} + L^f\varrho_M\sum_{s=1}^{n}\tilde{c}_{sk} - \gamma_k,$$

and

$$\zeta_k^* > \xi^h\sum_{s=1}^{n}\left(\hat{w}_{ks} - \check{w}_{ks}\right) + \xi^g\sum_{s=1}^{n}\sum_{l=1}^{m}\left(\hat{v}_{(l)ks} - \check{v}_{(l)ks}\right) + \varrho_M\xi^f\sum_{s=1}^{n}\left(\hat{c}_{ks} - \check{c}_{ks}\right), \quad k = 1, 2, \ldots, n, \tag{31}$$

then when the controller (30) is exerted on the slave MMNNs system (2), it can be synchronized with the MMNNs system (1) during the settling time, given by

$$t_2^* = \frac{\mathbb{V}(0)}{\Omega^*},$$

where $\Omega^* = \min_{1\le k\le n} \{\Omega_k^*\}$, and

$$\Omega_k^* = \zeta_k^* - \Big(\xi^h \sum_{s=1}^{n} \big(\hat{w}_{ks} - \check{w}_{ks}\big) + \xi^g \sum_{s=1}^{n}\sum_{l=1}^{m} \big(\hat{v}_{(l)ks} - \check{v}_{(l)ks}\big) + \varrho_M \xi^f \sum_{s=1}^{n} \big(\hat{c}_{ks} - \check{c}_{ks}\big)\Big),$$

and

$$\mathbb{V}(0) = \Big[\sum_{k=1}^{n} |e_k(0)| + \sum_{k=1}^{n}\sum_{s=1}^{n} \int_{-\varrho_M}^{0} L^f \tilde{c}_{ks} \int_{\vartheta}^{0} |e_s(x)| dx d\vartheta + \sum_{k=1}^{n}\sum_{s=1}^{n}\sum_{l=1}^{m} \frac{\tilde{v}_{(l)ks} L^g}{1-\tau_D} \int_{t-\tau_0}^{t} |e_s(x)| dx + \sum_{k=1}^{n} \frac{1}{2\varpi_k^*} \left(\varpi_k^*(0) - \varpi_k^*\right)^2 + \sum_{k=1}^{n} \frac{1}{2\zeta_k^*} \left(\zeta_k^*(0) - \zeta_k^*\right)^2\Big].$$

Proof: Under the controller (30), we construct the following Lyapunov-Krasovskii functional

$$\mathbb{V}(t) = \mathbb{V}_1(t) + \mathbb{V}_2(t) + \mathbb{V}_3(t) + \mathbb{V}_4(t), \tag{32}$$

where

$$\begin{aligned} \mathbb{V}_1(t) &= |e(t)|, \\ \mathbb{V}_2(t) &= \sum_{k=1}^{n}\sum_{s=1}^{n}\sum_{l=1}^{m} \frac{L^g \tilde{v}_{(l)ks}}{1-\tau_D} \int_{t-\tau_l(t)}^{t} |e_s(x)| dx, \\ \mathbb{V}_3(t) &= \sum_{k=1}^{n}\sum_{s=1}^{n} \int_{-\varrho(t)}^{0} \tilde{c}_{ks} L^f \int_{t+\vartheta}^{t} |e_s(x)| dx d\vartheta, \\ \mathbb{V}_4(t) &= \sum_{k=1}^{n} \frac{1}{2\varpi_k^*} \left(\varpi_k^*(t) - \varpi_k^*\right)^2 + \sum_{k=1}^{n} \frac{1}{2\zeta_k^*} \left(\zeta_k^*(t) - \zeta_k^*\right)^2. \end{aligned} \tag{33}$$

Based on the Chain rule introduced in [53], along the trajectory of (8), the derivative of $\mathbb{V}_1(t)$ can be calculated as

$$\begin{aligned} \dot{\mathbb{V}}_1(t) &= sign^T(e(t))\dot{e}(t) \\ &= sign^T(e(t))[-\Gamma e(t) + (\grave{W}(t) - \acute{W}(t))h(y(t)) \\ &\quad + \acute{W}(t)H(e(t)) + \sum_{l=1}^{m} (\grave{V}_l(t) - \acute{V}_l(t))g(y(t-\tau_l(t))) \\ &\quad + \sum_{l=1}^{m} \acute{V}_l(t)G(e(t-\tau_l(t))) + \acute{C}(t) \int_{t-\varrho(t)}^{t} F(e(x))dx \\ &\quad + (\grave{C}(t) - \acute{C}(t)) \int_{t-\varrho(t)}^{t} f(y(x))dx \\ &\quad + \mu(t)]. \end{aligned} \tag{34}$$

From Assumption 2, we can get that

$$\begin{aligned} & sign^T(e(t))\acute{W}(t)H(e(t)) \\ &\quad \le \sum_{k=1}^{n}\sum_{s=1}^{n} sign(e_k(t))\acute{w}_{ks}(t)h_s(e_s(t)) \\ &\quad \le \sum_{k=1}^{n}\sum_{s=1}^{n} |\acute{w}_{ks}(t)| \iota_s^h |e_s(t)| \\ &\quad \le L^h \sum_{k=1}^{n}\sum_{s=1}^{n} \tilde{w}_{sk} |e_k(t)|. \end{aligned} \tag{35}$$

Similar to (35), we can conclude that

$$\begin{aligned} & sign^T(e(t)) \sum_{l=1}^{m} \acute{V}_l(t) G\left(e\left(t-\tau_l(t)\right)\right) \\ &\quad = \sum_{k=1}^{n}\sum_{s=1}^{n}\sum_{l=1}^{m} sign\left(e_k(t)\right) \acute{v}_{(l)ks}(t) g_s(e_s(t-\tau_l(t))) \\ &\quad \le \sum_{k=1}^{n}\sum_{s=1}^{n}\sum_{l=1}^{m} sign\left(e_k(t)\right) \acute{v}_{(l)ks}(t) \iota_s^g |e_s\left(t-\tau_l(t)\right)| \\ &\quad \le L^g \sum_{k=1}^{n}\sum_{s=1}^{n}\sum_{l=1}^{m} \tilde{v}_{(l)ks} |e_s\left(t-\tau_l(t)\right)|, \end{aligned} \tag{36}$$

and

$$\begin{aligned} & sign^T(e(t))\acute{C}(t) \int_{t-\varrho(t)}^{t} F(e(x))dx \\ &\quad = \sum_{k=1}^{n}\sum_{s=1}^{n} sign\left(e_k(t)\right) \acute{c}_{ks}(t) \int_{t-\varrho(t)}^{t} f_s\left(e_s(x)\right) dx \\ &\quad \le \sum_{k=1}^{n}\sum_{s=1}^{n} \tilde{c}_{ks} \int_{t-\varrho(t)}^{t} \iota_s^f |e_s(x)| dx \\ &\quad \le L^f \sum_{k=1}^{n}\sum_{s=1}^{n} \tilde{c}_{ks} \int_{t-\varrho(t)}^{t} |e_s(x)| dx. \end{aligned} \tag{37}$$

According to Assumption 1, we otain

$$\begin{aligned} & sign^T(e(t)) \left(\grave{W}(t) - \acute{W}(t)\right) h(y(t)) \\ &\quad = \sum_{k=1}^{n}\sum_{s=1}^{n} sign\left(e_k(t)\right) \left(\grave{w}_{ks}(t) - \acute{w}_{ks}(t)\right) h_s(y_s(t)) \\ &\quad \le \sum_{k=1}^{n}\sum_{s=1}^{n} \left(\hat{w}_{ks} - \check{w}_{ks}\right) |sign\left(e_k(t)\right)| \xi_s^h \\ &\quad \le \xi^h \sum_{k=1}^{n}\sum_{s=1}^{n} \left(\hat{w}_{ks} - \check{w}_{ks}\right) \chi_k. \end{aligned} \tag{38}$$

Similar to (38), we can get

$$\begin{aligned} & sign^T(e(t)) \sum_{l=1}^{m} \left(\grave{V}_l(t) - \acute{V}_l(t)\right) g\Big(y\Big(t-\tau_l(t)\Big)\Big) \\ &\quad = \sum_{k=1}^{n}\sum_{s=1}^{n}\sum_{l=1}^{m} sign(e_k(t)) \Big(v_{(l)ks}(t) - \acute{v}_{(l)ks}(t)\Big) \\ &\qquad \cdot g_s\Big(y\Big(t-\tau_l(t)\Big)\Big) \\ &\quad \le \sum_{k=1}^{n}\sum_{s=1}^{n}\sum_{l=1}^{m} \left(\hat{v}_{(l)ks} - \check{v}_{(l)ks}\right) |sign\left(e_k(t)\right)| \xi_s^g \\ &\quad \le \xi^g \sum_{k=1}^{n}\sum_{s=1}^{n}\sum_{l=1}^{m} \left(\hat{v}_{(l)ks} - \check{v}_{(l)ks}\right) \chi_k. \end{aligned} \tag{39}$$

And we have

$$\begin{aligned} & sign^T(e(t))\left(\grave{C}(t)-\acute{C}(t)\right)\int_{t-\varrho(t)}^{t} f(y(x))dx \\ &= \sum_{k=1}^{n}\sum_{s=1}^{n} sign\,(e_k(t))\left(\grave{c}_{ks}(t)-\acute{c}_{ks}(t)\right)f_s(y_s(x))dx \\ &\le \sum_{k=1}^{n}\sum_{s=1}^{n}\left(\hat{c}_{ks}-\check{c}_{ks}\right)\int_{t-\varrho(t)}^{t}\xi_s^f dx \\ &\le \sum_{k=1}^{n}\sum_{s=1}^{n}\left(\hat{c}_{ks}-\check{c}_{ks}\right)\chi_k\int_{t-\varrho_M}^{t}\xi_s^f dx \\ &\le \varrho_M\xi^f\sum_{k=1}^{n}\sum_{s=1}^{n}\left(\hat{c}_{ks}-\check{c}_{ks}\right)\chi_k. \end{aligned} \tag{40}$$

On the other hand, we have

$$\begin{aligned} & sign^T(e(t))\left[-\Gamma e(t)+\mu(t)\right] \\ &= \sum_{k=1}^{n} sign\,(e_k(t))\left[-\gamma_k e_k(t)-\varpi_k^*(t)e_k\,(t)\right. \\ &\qquad \left.-\zeta_k^*(t)sign\,(e_k(t))\right] \\ &= \sum_{k=1}^{n}\left[-\gamma_k|e_k(t)|-\varpi_k^*(t)|e_k\,(t)\,|-\zeta_k^*(t)\chi_k\right]. \end{aligned} \tag{41}$$

Similarly, we calculate the derivatives of $\mathbb{V}_2(t)$, $\mathbb{V}_3(t)$, $\mathbb{V}_4(t)$ as follows:

$$\begin{aligned} \dot{\mathbb{V}}_2(t) &= \sum_{k=1}^{n}\sum_{s=1}^{n}\sum_{l=1}^{m}\frac{\tilde{v}_{(l)ks}L^g}{1-\tau_D}(|e_s(t)| \\ &\qquad -|e_s(t-\tau_l(t))|(1-\dot{\tau}_l(t))) \\ &\le L^g\sum_{k=1}^{n}\sum_{s=1}^{n}\sum_{l=1}^{m}\frac{\tilde{v}_{(l)sk}}{1-\tau_D}|e_k(t)| \\ &\qquad -L^g\sum_{k=1}^{n}\sum_{s=1}^{n}\sum_{l=1}^{m}\tilde{v}_{(l)ks}|e_s\,(t-\tau_l(t))\,|, \end{aligned} \tag{42}$$

$$\begin{aligned} \dot{\mathbb{V}}_3(t) &= \sum_{k=1}^{n}\sum_{s=1}^{n}\int_{-\varrho(t)}^{0}\tilde{c}_{ks}L^f\left(|e_s(t)|-|e_s(t+\vartheta)|\right)d\vartheta \\ &\le L^f\varrho_M\sum_{k=1}^{n}\sum_{s=1}^{n}\tilde{c}_{sk}|e_k(t)| \\ &\qquad -\sum_{k=1}^{n}\sum_{s=1}^{n}\tilde{c}_{ks}L^f\int_{t-\varrho(t)}^{t}|e_s(x)|dx, \end{aligned} \tag{43}$$

$$\begin{aligned} \dot{\mathbb{V}}_4(t) &= \sum_{k=1}^{n}\frac{1}{2\varpi_k^*}(\varpi_k^*(t)-\varpi_k^*)\dot{\varpi}(t) \\ &\qquad +\sum_{k=1}^{n}\frac{1}{2\zeta_k^*}\left(\zeta_k^*(t)-\zeta_k^*\right)\dot{\zeta}_k^*(t) \\ &= \sum_{k=1}^{n}\left(\varpi_k^*(t)-\varpi_k^*\right)|e_k(t)|+\sum_{k=1}^{n}\left(\zeta_k^*(t)-\zeta_k^*\right)\chi_k. \end{aligned} \tag{44}$$

Then from (34)-(44), we can obtain

$$\begin{aligned} \dot{\mathbb{V}}\,(t) &= \dot{\mathbb{V}}_1(t)+\dot{\mathbb{V}}_2(t)+\dot{\mathbb{V}}_3(t)+\dot{\mathbb{V}}_4(t) \\ &\le \sum_{k=1}^{n}\left(\sum_{s=1}^{n}L^h\tilde{w}_{sk}+L^g\sum_{s=1}^{n}\sum_{l=1}^{m}\frac{\tilde{v}_{(l)sk}}{1-\tau_D}-\varpi_k^*\right. \\ &\qquad \left.+L^f\varrho_M\sum_{s=1}^{n}\tilde{c}_{sk}-\gamma_k\right)|e_k(t)| \\ &\qquad +\sum_{k=1}^{n}\left(\xi^h\sum_{s=1}^{n}\left(\hat{w}_{ks}-\check{w}_{ks}\right)+\varrho_M\xi^f\sum_{s=1}^{n}\left(\hat{c}_{ks}-\check{c}_{ks}\right)\right. \\ &\qquad \left.+\xi^g\sum_{s=1}^{n}\sum_{l=1}^{m}\left(\hat{v}_{(l)ks}-\check{v}_{(l)ks}\right)-\zeta_k^*\right)\chi_k \\ &= -\sum_{k=1}^{n}\hbar_k^*|e_k(t)|-\sum_{k=1}^{n}\Omega_k^*\chi_k, \end{aligned} \tag{45}$$

where

$$\hbar_k^* = -\left[\sum_{s=1}^{n}L^h\tilde{w}_{sk}+L^g\sum_{s=1}^{n}\sum_{l=1}^{m}\frac{\tilde{v}_{(l)sk}}{1-\tau_D}-\varpi_k^* +L^f\varrho_M\sum_{s=1}^{n}\tilde{c}_{sk}-\gamma_k\right].$$

According to Theorem 2, we get the conclusion as follows

$$\dot{\mathbb{V}}(t) \le -\sum_{k=1}^{n}\Omega^*\chi_k < 0. \tag{46}$$

Apparently, the inequality (46) is similarity to (27), so the proving procedure behind is quite similar, so we omit the following proof process.

Remark 3: The synchronization criteria provided in Theorems 1 and 2 are both in the numerical form. We can further consider utilizing the linear matrix inequality (LMI) method to calculate them and study the synchronization problem of the delayed nonlinear system with which the synchronization criteria are much less conservative.

C. NON-LINEAR AND DELAY-DEPENDENT STATE-FEEDBACK CONTROLLER

In this subsection, we adopt a non-linear delay-dependent controller, given by

$$\begin{aligned} \mu(t) &= -sgn(e(t))\mathcal{P}|e(t)|-\sum_{l=1}^{m}sgn(e(t))\mathcal{Q}_l|e(t-\tau_l(t))| \\ &\qquad -sgn(e(t))\mathcal{H}\int_{t-\varrho(t)}^{t}|e(x)|dx-sgn(e(t))\mathcal{X} \\ &\qquad -\kappa sgn(e(t))|e(t)|^{\rho}, \end{aligned} \tag{47}$$

for $l = 1, 2, \ldots, m$, $\kappa > 0$ and $0 < \rho < 1$ are two known constants, $\mathcal{X} \in \mathbb{R}^n$ is a vector to be determined. Here we denote $sgn(e(t)) = diag(sign(e_1(t)), sign(e_2(t)), \ldots, sign(e_n(t)))$ and $|e(t)|^{\rho} = (|e_1(t)|^{\rho}, |e_2(t)|^{\rho}, \ldots, |e_n(t)|^{\rho})^T$. $\mathcal{P}$, $\mathcal{H}$, $\mathcal{Q}_l \in \mathbb{R}^{n\times n}$ are unknown matrices to be determined later.

Remark 4: The design of controller (47) is derived from the structure of the MMNNs model. It contains more free parameters, which is conducive to achieve the synchronization effect of the master-slave MMNNs systems (2) and (1).

Theorem 3: Suppose that the Assumptions 1 - 3 hold, and there exist $n\times n$-matrices $\mathcal{P}$, $\mathcal{Q}_l$, $\mathcal{H}$, and an appropriately designed vector $\mathcal{X}$, such that

$$\begin{aligned}
-\Gamma+L^h\widetilde{W}-\mathcal{P} &\leq 0,\\
L^g\widetilde{V}_l-\mathcal{Q}_l &\leq 0,\\
L^f\widetilde{C}-\mathcal{H} &\leq 0,\\
-\mathcal{X}\left(\hat{W}-\check{W}\right)\Xi^h+\varrho_M\left(\hat{C}-\check{C}\right)\Xi^f &\\
+\sum_{l=1}^{m}\left(\hat{V}_l-\check{V}_l\right)\Xi^g &\leq 0,
\end{aligned}$$

where $l = 1, 2, \ldots, m$, L^h, L^g, L^f, Ξ^h, Ξ^g and Ξ^f are described in Assumption 1. Then the MMNNs system (2) can be synchronized with (1) under the controller (47) during the settling time t_3^*, given by

$$t_3^* = \frac{2\left(\mathbb{V}(0)\right)^{\frac{1-\rho}{2}}}{k(1-\rho)}, \tag{48}$$

where $\mathbb{V}(0) = \frac{1}{2}e^T(0)e(0)$.

Proof: Construct the following Lyapunov functional $\mathbb{V}(t)$

$$\mathbb{V}(t) = \frac{1}{2}e^T(t)e(t). \tag{49}$$

Computing the derivative of $\mathbb{V}(t)$ along the trajectory of (8) leads to

$$\begin{aligned}
\dot{\mathbb{V}}(t) &= e^T(t)\dot{e}(t) = e^T(t)\Big[-\Gamma e(t)+(\grave{W}(t)-\acute{W}(t))h(y(t))\\
&\quad+\acute{W}(t)H(e(t))+\sum_{l=1}^{m}(\grave{V}_l(t)-\acute{V}_l(t))g(y(t-\tau_l(t)))\\
&\quad+\sum_{l=1}^{m}\acute{V}_l(t)G(e(t-\tau_l(t)))+\acute{C}(t)\int_{t-\varrho(t}^{t}F(e(x)dx\\
&\quad+(\grave{C}(t)-\acute{C}(t))\int_{t-\varrho(t)}^{t}f(y(x))dx+\mu(t)\Big].
\end{aligned} \tag{50}$$

We can easily conclude

$$e^T(t)\left[-\Gamma e(t)\right] = -|e(t)|^T\Gamma|e(t)|. \tag{51}$$

From Assumption 2, it follows

$$\begin{aligned}
e^T(t)\acute{W}(t)H(e(t)) &\leq |e(t)|^T|\acute{W}(t)|L^h|e(t)|\\
&\leq L^h|e(t)|^T\widetilde{W}|e(t)|.
\end{aligned} \tag{52}$$

Similarly, we can get

$$\begin{aligned}
&e^T(t)\sum_{l=1}^{m}\acute{V}_l(t)G(e(t-\tau_l(t)))\\
&\quad\leq |e(t)|^T\sum_{l=1}^{m}|\acute{V}_l(t)|L^g|e(t-\tau_l(t))|\\
&\quad\leq |e(t)|^TL^g\sum_{l=1}^{m}\widetilde{V}_l|e(t-\tau_l(t))|.
\end{aligned} \tag{53}$$

And we have

$$\begin{aligned}
&e^T(t)\acute{C}(t)\int_{t-\varrho(t)}^{t}F(e(x))dx\\
&\qquad\leq L^f|e(t)|^T\widetilde{C}\int_{t-\varrho(t)}^{t}|e(s)|ds.
\end{aligned} \tag{54}$$

From Assumptions 1 and 3, it implies that

$$\begin{aligned}
&e^T(t)\Big(\grave{C}(t)-\acute{C}(t)\Big)\int_{t-\varrho(t)}^{t}f(y(x))dx\\
&\quad\leq |e(t)|^T\left(\hat{C}-\check{C}\right)\int_{t-\varrho(t)}^{t}\Xi^f ds\\
&\quad\leq |e(t)|^T\varrho_M\left(\hat{C}-\check{C}\right)\Xi^f.
\end{aligned} \tag{55}$$

Similar to (55), we have

$$\begin{aligned}
&e^T(t)\sum_{l=1}^{m}\left(\grave{V}_l(t)-\acute{V}_l(t)\right)g(y(t-\tau_l(t)))\\
&\qquad\leq |e(t)|^T\sum_{l=1}^{m}\left(\hat{V}_l-\check{V}_l\right)\Xi^g.
\end{aligned} \tag{56}$$

And

$$e^T(t)(\grave{W}(t)-\acute{W}(t))h(y(t)) \leq |e(t)|^T\left(\hat{W}-\check{W}\right)\Xi^h. \tag{57}$$

On the other hand, we have

$$\begin{aligned}
&e^T(t)\mu(t)\\
&= -|e(t)|^T\mathcal{P}|e(t)|-\sum_{l=1}^{m}|e(t)|^T\mathcal{Q}_l|e(t-\tau_l(t))|\\
&\quad-|e(t)|^T\mathcal{H}\int_{t-\varrho(t)}^{t}|e(s)|ds-|e(t)|^T\mathcal{X}-\kappa|e(t)|^T|e(t)|^\rho.
\end{aligned} \tag{58}$$

From (51) to (58), we conclude

$$\begin{aligned}
\dot{\mathbb{V}}(t) &\leq |e(t)|^T\left(-\Gamma+L^h\widetilde{W}-\mathcal{P}\right)|e(t)|\\
&\quad+|e(t)|^T\sum_{l=1}^{m}\left(L^g\widetilde{V}_l-\mathcal{Q}_l\right)|e(t-\tau_l(t))|\\
&\quad+|e(t)|^T\left(L^f\widetilde{C}-\mathcal{H}\right)\int_{t-\varrho(t)}^{t}|e(s)|ds\\
&\quad-\kappa\sum_{k=1}^{n}|e_k(t)|^{\rho+1}+|e(t)|^T\Big(\left(\hat{W}-\check{W}\right)\Xi^h\\
&\quad+\varrho_M\left(\hat{C}-\check{C}\right)\Xi^f+\sum_{l=1}^{m}\left(\hat{V}_l-\check{V}_l\right)\Xi^g-\mathcal{X}\Big).
\end{aligned} \tag{59}$$

According to Theorem 3, Lemma 2, and (59) we can get

$$\begin{aligned}
\dot{\mathbb{V}}(t) &\leq -\kappa\sum_{k=1}^{n}|e_k(t)|^{\rho+1} \leq -\kappa\cdot 2^{\frac{\rho+1}{2}}(\mathbb{V}(t))^{\frac{\rho+1}{2}}\\
&\leq -\kappa(\mathbb{V}(t))^{\frac{\rho+1}{2}}.
\end{aligned} \tag{60}$$

From (60) and Lemma 1, we can conclude that under the controller (47), the MMNNs systems (2) and (1) can obtain finite-time synchronization during the settling time t_3^*, which can be calculated by using (48).

Hence, the proof of Theorem 3 is completed.

Corollary 2: For master-slave MMNNs systems (2) and (1), if $m = 1$, the MMNNs systems degenerate into single-linked MNNs systems. Under this condition, if $\mathcal{P}$, $\mathcal{Q}_1$, $\mathcal{H}$ and $\mathcal{X}$ meet the following requirements:

$$\mathcal{P} \geq L^h\widetilde{W}-\Gamma,\ \mathcal{Q}_1 \geq L^g\widetilde{V}_1,\ \mathcal{H} \geq L^f\widetilde{C},$$
$$\mathcal{X}\left(\hat{W}-\check{W}\right)\Xi^h-\varrho_M\left(\hat{C}-\check{C}\right)\Xi^f-\left(\hat{V}_1-\check{V}_1\right)\Xi^g \geq 0,$$

then MNNs systems (1) and (2) with $m = 1$ can gain finte-time synchronization within a calculated time, which can be calculated by using (48) with $m = 1$.

Proof: The proof process is similar to that of Theorem 3, hence, we omit the proof process here.

Remark 5: Corollary 2 can be viewed as a special case of Theorem 3, since there is only one link between any two nodes of the MMNNs systems.

Remark 6: Theorem 1 adopts a linear and delay-independent state-feedback controller, Theorem 2 uses a non-linear adaptive and delay-dependent controller, Theorem 3 utilizes a non-linear and delay-independent state-feedback controllers. The former two controllers adopted are simpler, but they need more assumptions in the proof procedures. The last controller adopted is more complex, while it requires fewer hypothetical prerequisites. Hence, the last one is more conservative.

Remark 7: Because different controllers are adopted in deriving Theorems 1, 2, and 3, different synchronization criteria are obtained. From these criteria, we can conclude that because the form of controller (47) is more complex, so the criterion of Theorem 3 is simpler than those of Theorems 1 and 2.

Remark 8: The controllers (9), (30) and (47) contain discontinuous terms $sign(e_i(t))$ or $sign(e(t))$ which might lead to chatting phenomenon, which largely exists in practical engineering application. Therefore, we must take effective measures to avoid this situation. In this paper, we mainly use an approximate value $\frac{e_i(t)}{|e_i(t)|+\Lambda}$ to replace $sign(e_i(t))$, in which Λ is a known small enough positive constant. However, this replacement is not made in the process of theoretical derivation in this paper, because it may cause confusion.

Remark 9: Xiaoyang Liu *et al.* studied the finite-time synchronization problem in Refs. [56], [57] and obtained some interesting results. In Ref. [56], the problem of finite-time consensus of multi-agent systems was investigated, and a centralized switching consensus protocol was designed to realize the finite-time consensus. The finite-time synchronization problem of nonlinear coupled neural networks was investigated by designing a new switching pinning controller in Ref. [57]. The above results used switching control, and in this paper we use adaptive state-feedback control. In addition, the research models are different.

IV. NUMERICAL SIMULATIONS

Consider the following master MMNNs system:

$$\begin{aligned}\dot{z}_k(t) = &-\gamma_k z_k(t)+\sum_{s=1}^{2} w_{ks}(z_k(t))h_s(z_s(t))\\ &+\sum_{s=1}^{2}\sum_{l=1}^{2} v_{(l)ks}(z_k(t))g_s(z_s(t-\tau_l(t)))\\ &+\sum_{s=1}^{2} c_{ks}(z_k(t))\int_{t-\varrho(t)}^{t} f_s(z_s(x))dx+J_k,\quad t \geq 0, \quad (61)\end{aligned}$$

The corresponding slave MMNNs system is given as

$$\begin{aligned}\dot{y}_k(t) = &-\gamma_k y_k(t)+\sum_{s=1}^{2} w_{ks}(y_k(t))h_s(y_s(t))\\ &+\sum_{s=1}^{2}\sum_{l=1}^{2} v_{(l)ks}(y_k(t))g_s(y_s(t-\tau_l(t)))\\ &+\sum_{s=1}^{2} c_{ks}(y_k(t))\int_{t-\varrho(t)}^{t} f_s(y_s(x))dx\\ &+J_k(t)+\mu_k(t),\quad t \geq 0. \quad (62)\end{aligned}$$

$k = 1, 2$, and we set $\mho_1 = \mho_2 = 1$, and the weights of $w_{ks}(\cdot)$, $v_{(l)ks}(\cdot)$, and $c_{ks}(\cdot)$ for $s = 1, 2$ are given by

$$w_{11}(x_1(t)) = \begin{cases}-3.28, & |x_1(t)| > 1,\\ 1.99, & |x_1(t)| \leq 1,\end{cases}$$

$$w_{12}(x_1(t)) = \begin{cases}0.95, & |x_1(t)| > 1,\\ -1.2, & |x_1(t)| \leq 1,\end{cases}$$

$$w_{21}(x_2(t)) = \begin{cases}0.25, & |x_2(t)| > 1,\\ -0.85, & |x_2(t)| \leq 1,\end{cases}$$

$$w_{22}(x_2(t)) = \begin{cases}-1.78, & |x_2(t)| > 1,\\ 2.26, & |x_2(t)| \leq 1,\end{cases}$$

$$v_{(1)11}(x_1(t)) = \begin{cases}0.88, & |x_1(t)| > 1,\\ -1.92, & |x_1(t)| \leq 1,\end{cases}$$

$$v_{(1)12}(x_1(t)) = \begin{cases}1.15, & |x_1(t)| > 1,\\ -1.24, & |x_1(t)| \leq 1,\end{cases}$$

$$v_{(1)21}(x_2(t)) = \begin{cases}-1.68, & |x_2(t)| > 1,\\ 1.56, & |x_2(t)| \leq 1,\end{cases}$$

$$v_{(1)22}(x_2(t)) = \begin{cases}1.45, & |x_2(t)| > 1,\\ -1.8, & |x_2(t)| \leq 1,\end{cases}$$

$$v_{(2)11}(x_1(t)) = \begin{cases}0.88, & |x_1(t)| > 1,\\ -1.99, & |x_1(t)| \leq 1,\end{cases}$$

$$v_{(2)12}(x_1(t)) = \begin{cases}-1.15, & |x_1(t)| > 1,\\ -2.24, & |x_1(t)| \leq 1,\end{cases}$$

$$v_{(2)21}(x_2(t)) = \begin{cases}-0.68, & |x_2(t)| > 1,\\ 0.56, & |x_2(t)| \leq 1,\end{cases}$$

$$v_{(2)22}(x_2(t)) = \begin{cases} 0.95, & |x_2(t)| > 1, \\ -1.17, & |x_2(t)| \le 1, \end{cases}$$

$$c_{11}(x_1(t)) = \begin{cases} -1.88, & |x_2(t)| > 1, \\ -0.89, & |x_2(t)| \le 1, \end{cases}$$

$$c_{12}(x_1(t)) = \begin{cases} -0.98, & |x_2(t)| > 1, \\ 1.15, & |x_2(t)| \le 1, \end{cases}$$

$$c_{21}(x_2(t)) = \begin{cases} 2.56, & |x_2(t)| > 1, \\ -1.76, & |x_2(t)| \le 1, \end{cases}$$

$$c_{22}(x_2(t)) = \begin{cases} -2.35, & |x_2(t)| > 1, \\ -0.85, & |x_2(t)| \le 1 \end{cases}$$

where $x_k(t)$ represents $z_k(t)$ or $y_k(t)$.

We choose the following activation functions, $f(z) = h(z) = g(z) = \frac{|z+1|-|z-1|}{2}$, it can be concluded that $|h(z)| = |f(z)| = |g(z)| \le 1$. According to Assumption 1, we can get $\Xi^h = \Xi^g = \Xi^f = (1,1)^T$. Besides, we can calculate the derivatives of $h(z)$, $g(z)$ and $f(z)$, and get $\dot{h}(z) = \dot{g}(z) = \dot{f}(z) = \frac{1}{2}(sign(z+1)-sign(z-1))$, calculating their derivatives and get that their values are smaller than 1. According to Assumption 2, we conclude that $L^h = L^g = L^f = 1$.

The time-varying delays and distributed delay are chosen as: $\tau_1(t) = 0.5+0.5cos(t)$, and $\tau_2(t) = \varrho(t) = 0.5+0.5sin(t)$, from which we can conclude that $\tau = 1$, $\tau_D = 0.5$, $\varrho_M = 1$ and $\varrho_D = 0.5$.

We choose $J = (sin(t), cos(t))^T$, and the initial values are chosen as $x(0) = (0.4, 0.6)^T$, $y(0) = (5, 2)^T$, $t \in [-1, 0]$. Thus, we can obtain that $e(0) = (4.6, 1.4)^T$.

Next we give the following three simulation examples to verify the effectiveness of Theorems 1, 2, and 3.

Example 1: This simulation is conducted to verify the effectiveness of Theorem 1 (see III-A). When there are no controller exerted on the MMNNs system (62), the state curves of $z_1(t)$, $y_1(t)$, and $z_2(t)$, $y_2(t)$ are shown in Figs. 1 and 2, respectively. Fig. 3 shows the error curves of $e_1(t)$ and $e_2(t)$ between the MMNNs (61) and (62).

According to Theorem 1, we can get $\underline{\varpi} \ge 20.09$, $\underline{\zeta} > 23.69$, so we take the following system parameters, $\varpi_1 = 21, \varpi_2 = 22$, $\zeta_1 = 25$ and $\zeta_2 = 24$, respectively, thus get the following controller

$$\begin{cases} \mu_1(t) = -21e_1(t)-25sign(e_1(t)), \\ \mu_2(t) = -22e_2(t)-24sign(e_2(t)). \end{cases} \tag{63}$$

We caluculate the settling time and get $t_1^* = 15.555$. The state curves of $z_1(t)$, $y_1(t)$, and $z_2(t)$, $y_2(t)$ are shown in Figs. 4 and 5, respectively. Fig. 6 describes the error state curves of $e_1(t)$, $e_2(t)$ between MMNNs systems (61) and (62).

Remark 10: Comparing Figs. 6 with 3, we can obtain that MMNNs systems (62) and (61) realize finite-time synchronization during t_1^* since the error curves of $e_1(t)$, $e_2(t)$ tend to zero in 0.5 second as shown in Fig. 6, which verify the correctness of the criterion proposed in Theorem 1.

Example 2: This simulation is conducted to verify Theorem 2 (see III-B). According to Theorem 2, we can get $\omega_1^* \ge 16.61, \omega_2^* \ge 17.36$, $\zeta_1^* > 19.69$, and $\zeta_2^* > 20.81$, so we choose $\omega_1^* = 17, \omega_2^* = 18$, $\zeta_1^* = 20$ and $\zeta_2^* = 21$, respectively. Calculating the settling time and get $t_2^* = 754.58$. The state trajectory curves of $z_1(t)$, $y_1(t)$, $z_2(t)$, and $y_2(t)$ are described by Figs. 7 and 8, respectively.

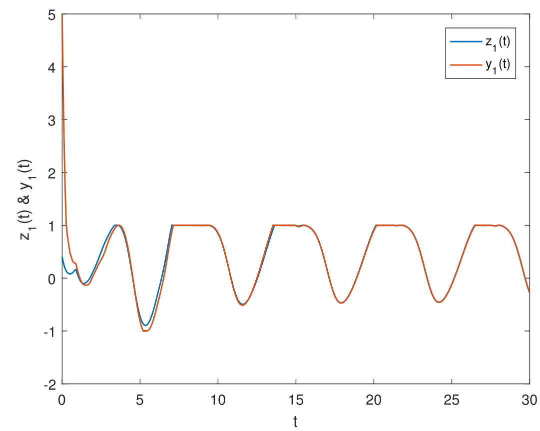

FIGURE 1. **The state curves of $z_1(t)$ and $y_1(t)$ with initial value $z_1(0) = 0.4, y_1(0) = 5$ without controller.**

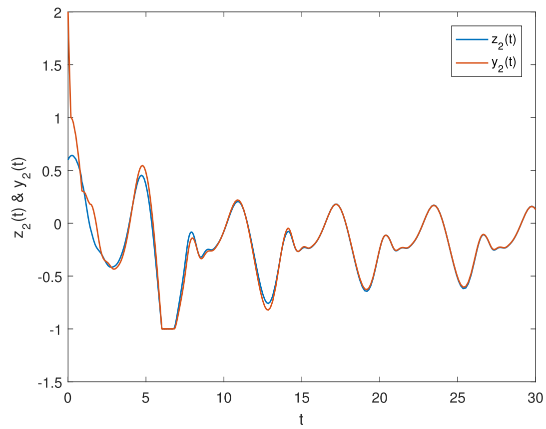

FIGURE 2. **The state curves of $z_2(t)$ and $y_2(t)$ with initial value $z_2(0) = 0.6, y_2(0) = 2$ without controller.**

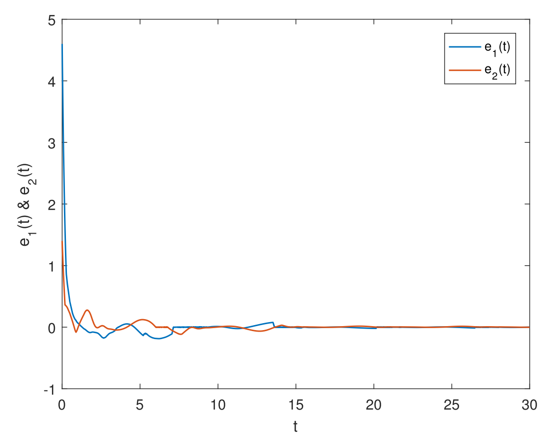

FIGURE 3. **The error state curves of $e_1(t)$ and $e_2(t)$ with initial value $e(0) = (4.6, 1.4)^T$ without controller.**

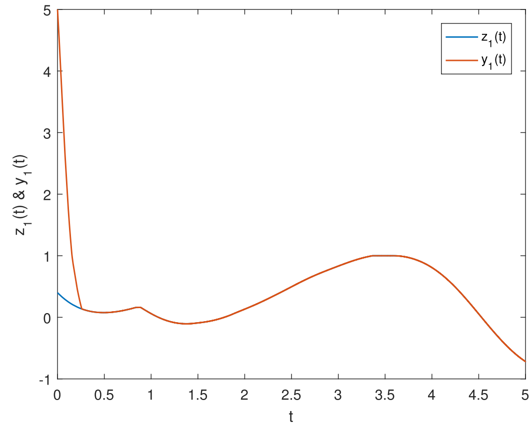

FIGURE 4. **The state trajectory curves of $z_1(t)$ and $y_1(t)$ with initial value $z_1(0) = 0.4, y_1(0) = 5$ under the controller (63).**

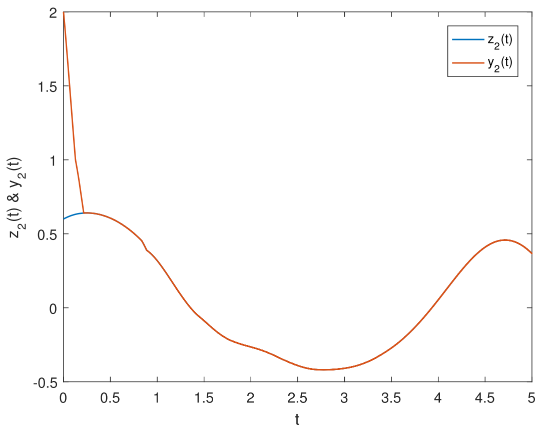

FIGURE 5. **The state trajectory curves of $z_2(t)$ and $y_2(t)$ with initial values $z_2(0) = 0.6, y_2(0) = 2$ under the controller (63).**

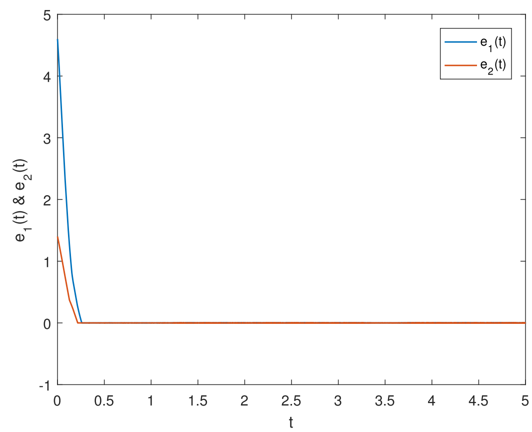

FIGURE 6. **The error state curves of $e_1(t)$ and $e_2(t)$ with initial value $e(0) = (4.6, 1.4)^T$ under the controller (63).**

Fig. 9 describes the trajectory curves of the errors $e_1(t)$ and $e_2(t)$. By analyzing Fig. 9, we conclude that MMNNs systems (62) and (61) realize synchronization during t_2^* since the error curves of $e_1(t), e_2(t)$ tend to zero in 0.5 second as shown in Fig. 9, that verify the correctness of the method proposed in Theorem 2.

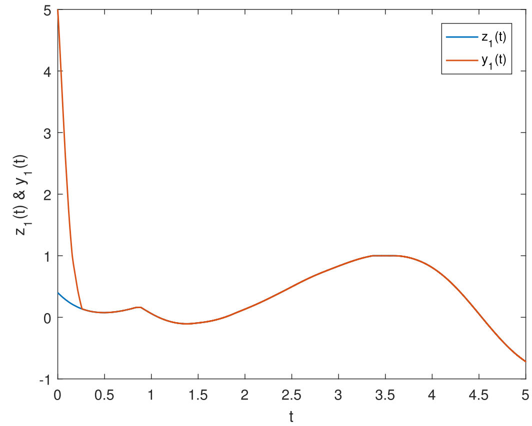

FIGURE 7. **The state curves of $z_1(t)$ and $y_1(t)$ with initial values $z_1(0) = 0.4, y_1(0) = 5$ under the controller (30).**

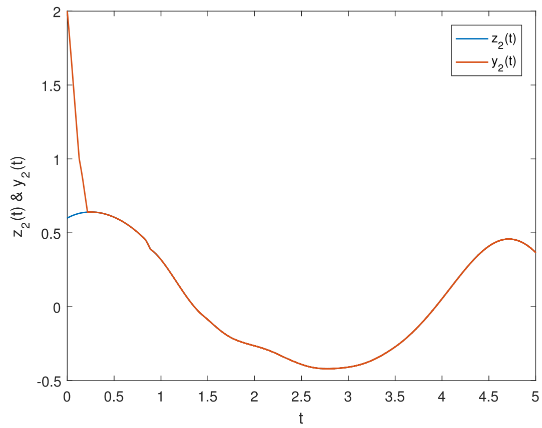

FIGURE 8. **The state curves of $z_2(t)$ and $y_2(t)$ with initial values $z_2(0) = 0.6, y_2(0) = 2$ under the controller (30).**

Remark 11: Besides, the settling time $t_2^*$is so big because we choose relatively small control gains $\zeta_1^* = 20, \zeta_2^* = 21$, and obtain $\Omega^* = 0.19$, which makes the settling time $\frac{\mathbb{V}(0)}{\Omega^*}$ really big. But in real-world engineering applications, the synchronization time is very short which we can conclude from Fig. 9. According to Theorem 2, we conclude that t_2^* is strongly associated with the model parameters and initial conditions of MMNNs systems, and in most of the time, it is really hard to implent because gaining all parameters in adance is very hard.

Example 3: This simulation is carried out to verify the effectiveness of Theorem 3 (see III-C).

According to the synchronization criterion proposed in Theorem 3, we set the following controller parameters:

$$\mathcal{P} = \begin{pmatrix} -1.22 & 1.2 \\ 0.85 & -0.24 \end{pmatrix}, \quad \mathcal{Q}_1 = \begin{pmatrix} 1.92 & 1.24 \\ 1.68 & 1.8 \end{pmatrix},$$
$$\mathcal{Q}_2 = \begin{pmatrix} 1.99 & 2.24 \\ 0.68 & 1.17 \end{pmatrix}, \quad \mathcal{H} = \begin{pmatrix} 1.88 & 1.15 \\ 2.56 & 2.35 \end{pmatrix},$$

and

$$\mathcal{X} = \begin{pmatrix} 19.69 \\ 20.81 \end{pmatrix}.$$

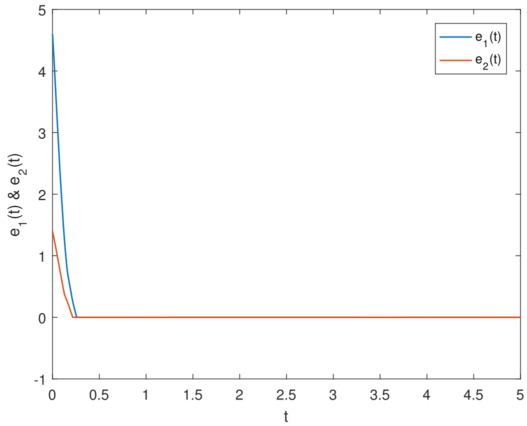

FIGURE 9. The error state curves of $e_1(t)$ and $e_2(t)$ with initial value $e(0) = (4.6, 1.4)^T$ under the controller (30).

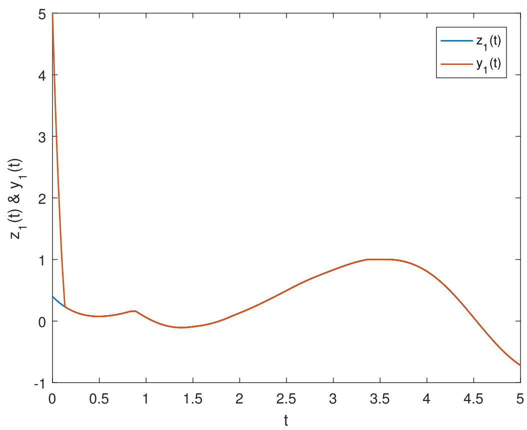

FIGURE 10. The first dimensional state trajectory curves of $z_1(t)$ and $y_1(t)$ with initial value $z_1(0) = 0.4, y_1(0) = 5$ under the controller (47).

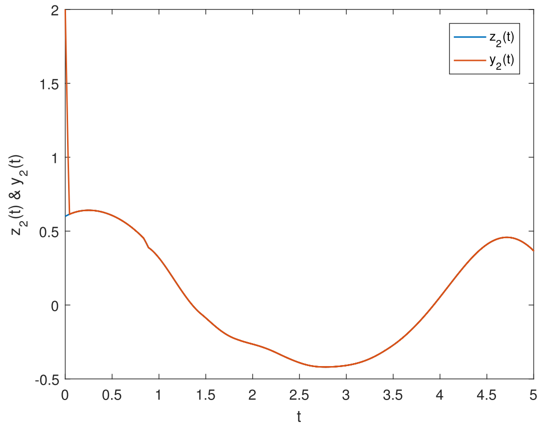

FIGURE 11. The second dimensional state trajectory curves of $z_2(t)$ and $y_2(t)$ with initial values $z_2(0) = 0.6, y_2(0) = 2$ under the controller (47).

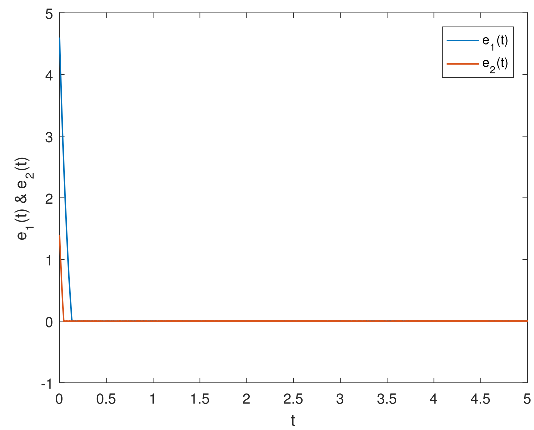

FIGURE 12. The error state curves of $e_1(t)$ and $e_2(t)$ with initial value $e(0) = (4.6, 1.4)^T$ under the controller (47).

Furthermore, we choose $\kappa = 1$, $\rho = 0.68$, and calculate the settling time and get $t_3^* = 9.246$. The state trajectory curves of $z_1(t)$, $y_1(t)$, and $z_2(t)$, $y_2(t)$ are shown in Figs. 10 and 11, respectivey. Fig. 12 describes the trajectory curves of the errors $e_1(t)$, $e_2(t)$ between the MMNNs systems (61) and (62).

Remark 12: Comparing Figs. 12 with 3, we conclude that MMNNs systems (62) and (61) realize synchronization during t_3^*, since the error curves $e_1(t)$, $e_2(t)$ tend to zero in Fig. 12, which verifies the correctness of the method proposed in Theorem 3. Comparing Figs. 12 and 6, we can easily conclude that the more complex the controller is, the longer time needed to obtain synchronization from analyzing the results of Figs. 12 and 6. However, the controller (47) needs more constraints while the controller (63) is much less conservative. In the actual engineering environment, it is very hard to find the appropriate activation functions which satisfy all the constraints, and in the neural networks, it is very hard to mimic the actual activation functions. Hence, we have to choose between the time cost and the conservativeness.

Remark 13: Comparing Figs. 12, 9, 6 with 3, we arrival at a conclusion that although MMNNs systems (62) and (61) can obtain finite-time synchronization in 15 seconds without any controller, the convergence time is too long to satisfy the requirements of real-world applications, such as secure communication. When the controllers (63), (30), and (47) are added to the MMNNs system (62), the MMNN systems (62) and (61) can achieve synchronization within 0.5 second, which greately shorten the convergence time and could be applied in secure communication.

V. CONCLUSION AND FUTURE WORK

Based on the concept of master-slave, in our paper, the synchronization and stabilization problem of the MMNNs systems is investigated over a finite time interval. We design three different state-feedback controllers to obtain the finite-time synchronization between master and slave MMNNs systems. The first one is a linear and delay-dependent state-feedback controller, the second one is a non-linear adaptive and delay-independent state-feedback controller, and the last one is non-linear and delay-dependent state-feedback controller. By utilizing the proposed controllers, sufficient criteria are derived to ensure the finite-time synchronization of the proposed MMNNs systems. Three different numerical simulations are presented to validate the correctness and the feasibility of the obtained theoretical criteria. Our future work will focus on the investigation of the finite-time synchronization and stability of the multi-linked memristor-based bidirectional associative memory (BAM) neural networks with mixed time-varying delays.

REFERENCES

[1] L. Chua, "Memristor–The missing circuit element," *IEEE Trans. Circuit Theory*, vol. 18, no. 5, pp. 507–519, 1971.
[2] S. Bhattacharjee, R. Wigchering, H. G. Manning, J. J. Boland, and P. K. Hurley, "Emulating synaptic response in n-and p-channel MoS_2 transistors by utilizing charge trapping dynamics," *Sci. Rep.*, vol. 10, no. 1, pp. 1–8, Dec. 2020.
[3] D. B. Strukov, G. S. Snider, D. R. Stewart, and R. S. Williams, "The missing memristor found," *Nature*, vol. 453, no. 7191, p. 80, 2008.
[4] M. J. Sharifi and Y. M. Banadaki, "General spice models for memristor and application to circuit simulation of memristor-based synapses and memory cells," *J. Circuits, Syst. Comput.*, vol. 19, no. 2, pp. 407–424, Apr. 2010.
[5] R. Li and H. Wei, "Synchronization of delayed Markovian jump memristive neural networks with reaction–diffusion terms via sampled data control," *Int. J. Mach. Learn. Cybern.*, vol. 7, no. 1, pp. 157–169, Feb. 2016.
[6] C. Chen, L. Li, H. Peng, Y. Yang, L. Mi, and L. Wang, "A new fixed-time stability theorem and its application to the synchronization control of memristive neural networks," *Neurocomputing*, vol. 349, pp. 290–300, Jul. 2019.
[7] S. Liu, Y. Yu, S. Zhang, and Y. Zhang, "Robust stability of fractional-order memristor-based Hopfield neural networks with parameter disturbances," *Phys. A, Stat. Mech. Appl.*, vol. 509, pp. 845–854, Nov. 2018.
[8] Y. Cao, Y. Cao, S. Wen, T. Huang, and Z. Zeng, "Passivity analysis of delayed reaction–diffusion memristor-based neural networks," *Neural Netw.*, vol. 109, pp. 159–167, Jan. 2019.
[9] Q. Xiao, Z. Huang, and Z. Zeng, "Passivity analysis for memristor-based inertial neural networks with discrete and distributed delays," *IEEE Trans. Syst., Man, Cybern., Syst.*, vol. 49, no. 2, pp. 375–385, Feb. 2019.
[10] Q. Xiao, T. Huang, and Z. Zeng, "Passivity and passification of fuzzy memristive inertial neural networks on time scales," *IEEE Trans. Fuzzy Syst.*, vol. 26, no. 6, pp. 3342–3355, Dec. 2018.
[11] J.-L. Wang, X.-X. Zhang, H.-N. Wu, T. Huang, and Q. Wang, "Finite-time passivity and synchronization of coupled reaction–diffusion neural networks with multiple weights," *IEEE Trans. Cybern.*, vol. 49, no. 9, pp. 3385–3397, Sep. 2019.
[12] H. Wei, C. Chen, Z. Tu, and N. Li, "New results on passivity analysis of memristive neural networks with time-varying delays and reaction–diffusion term," *Neurocomputing*, vol. 275, pp. 2080–2092, Jan. 2018.
[13] Y. Fan, X. Huang, Z. Wang, and Y. Li, "Global dissipativity and quasi-synchronization of asynchronous updating fractional-order memristor-based neural networks via interval matrix method," *J. Franklin Inst.*, vol. 355, no. 13, pp. 5998–6025, Sep. 2018.
[14] S. Ding, Z. Wang, and H. Zhang, "Dissipativity analysis for stochastic memristive neural networks with time-varying delays: A discrete-time case," *IEEE Trans. Neural Netw. Learn. Syst.*, vol. 29, no. 3, pp. 618–630, Mar. 2018.
[15] Z. Tu, N. Ding, Y. Feng, L. Zou, W. Zhang, and L. Li, "Adaptive synchronization of memristive neural networks with time-varying delays and reaction–diffusion term," *Appl. Math. Comput.*, vol. 311, pp. 118–128, Oct. 2017.
[16] Y. Zhou, C. Li, L. Chen, and T. Huang, "Global exponential stability of memristive Cohen–Grossberg neural networks with mixed delays and impulse time window," *Neurocomputing*, vol. 275, pp. 2384–2391, Jan. 2018.
[17] Y. Zhao, J. Kurths, and L. Duan, "Input-to-State stability analysis for memristive Cohen-Grossberg-type neural networks with variable time delays," *Chaos, Solitons Fractals*, vol. 114, pp. 364–369, Sep. 2018.
[18] L. Zhang, Y. Yang, and X. Xu, "Synchronization analysis for fractional order memristive Cohen–Grossberg neural networks with state feedback and impulsive control," *Phys. A, Stat. Mech. Appl.*, vol. 506, pp. 644–660, Sep. 2018.
[19] X. Yao, S. Zhong, T. Hu, H. Cheng, and D. Zhang, "Uniformly stable and attractive of fractional-order memristor-based neural networks with multiple delays," *Appl. Math. Comput.*, vol. 347, pp. 392–403, Apr. 2019.
[20] M. Zheng, L. Li, H. Peng, J. Xiao, Y. Yang, Y. Zhang, and H. Zhao, "Finite-time stability and synchronization of memristor-based fractional-order fuzzy cellular neural networks," *Commun. Nonlinear Sci. Numer. Simul.*, vol. 59, pp. 272–291, Jun. 2018.
[21] Y. Zhang, Y. Yu, and X. Cui, "Dynamical behaviors analysis of memristor-based fractional-order complex-valued neural networks with time delay," *Appl. Math. Comput.*, vol. 339, pp. 242–258, Dec. 2018.
[22] L. Zhang and Y. Yang, "Different impulsive effects on synchronization of fractional-order memristive BAM neural networks," *Nonlinear Dyn.*, vol. 93, no. 2, pp. 233–250, Jul. 2018.
[23] C. Rajivganthi, F. A. Rihan, S. Lakshmanan, R. Rakkiyappan, and P. Muthukumar, "Synchronization of memristor-based delayed BAM neural networks with fractional-order derivatives," *Complexity*, vol. 21, no. S2, pp. 412–426, Nov. 2016.
[24] H. Cheng, S. Zhong, Q. Zhong, K. Shi, and X. Wang, "Lag exponential synchronization of delayed memristor-based neural networks via robust analysis," *IEEE Access*, vol. 7, pp. 173–182, 2019.
[25] X. Wang, K. She, S. Zhong, and H. Yang, "Lag synchronization analysis of general complex networks with multiple time-varying delays via pinning control strategy," *Neural Comput. Appl.*, vol. 31, no. 1, pp. 43–53, Jan. 2019.
[26] L. Zhang, Y. Yang, F. Wang, and X. Sui, "Lag synchronization for fractional-order memristive neural networks with time delay via switching jumps mismatch," *J. Franklin Inst.*, vol. 355, no. 3, pp. 1217–1240, Feb. 2018.
[27] N. Durga and P. Muthukumar, "Existence and exponential behavior of multi-valued nonlinear fractional stochastic integro-differential equations with Poisson jumps of Clarke's subdifferential type," *Math. Comput. Simul.*, vol. 155, pp. 347–359, Jan. 2019.
[28] Z. Wang and X. Liu, "Exponential stability of impulsive complex-valued neural networks with time delay," *Math. Comput. Simul.*, vol. 156, pp. 143–157, Feb. 2019.
[29] A. Perasso, "Global stability and uniform persistence for an infection load-structured Si model with exponential growth velocity," *Commun. Pure Appl. Anal.*, vol. 18, no. 1, pp. 15–32, 2019.
[30] L. Socha and Q. Zhu, "Exponential stability with respect to part of the variables for a class of nonlinear stochastic systems with Markovian switchings," *Math. Comput. Simul.*, vol. 155, pp. 2–14, Jan. 2019.
[31] A. Abdurahman, "New results on the general decay synchronization of delayed neural networks with general activation functions," *Neurocomputing*, vol. 275, pp. 2505–2511, Jan. 2018.
[32] A. Abdurahman and H. Jiang, "Nonlinear control scheme for general decay projective synchronization of delayed memristor-based BAM neural networks," *Neurocomputing*, vol. 357, pp. 282–291, Sep. 2019.
[33] J. L. Mata-Machuca and R. Aguilar-López, "Adaptative synchronization in multi-output fractional-order complex dynamical networks and secure communications," *Eur. Phys. J. Plus*, vol. 133, no. 1, p. 14, Jan. 2018.
[34] S. Jia, C. Hu, J. Yu, and H. Jiang, "Asymptotical and adaptive synchronization of Cohen–Grossberg neural networks with heterogeneous proportional delays," *Neurocomputing*, vol. 275, pp. 1449–1455, Jan. 2018.
[35] D. Zhang, J. Cheng, J. Cao, and D. Zhang, "Finite-time synchronization control for semi-Markov jump neural networks with mode-dependent stochastic parametric uncertainties," *Appl. Math. Comput.*, vols. 344–345, pp. 230–242, Mar. 2019.
[36] R. Sakthivel, S. Kanakalakshmi, B. Kaviarasan, Y.-K. Ma, and A. Leelamani, "Finite-time consensus of input delayed multi-agent systems via non-fragile controller subject to switching topology," *Neurocomputing*, vol. 325, pp. 225–233, Jan. 2019.
[37] L. Wang, T. Dong, and M.-F. Ge, "Finite-time synchronization of memristor chaotic systems and its application in image encryption," *Appl. Math. Comput.*, vol. 347, pp. 293–305, Apr. 2019.
[38] X. Yang, J. Cao, and J. Liang, "Exponential synchronization of memristive neural networks with delays: Interval matrix method," *IEEE Trans. Neural Netw. Learn. Syst.*, vol. 28, no. 8, pp. 1878–1888, Aug. 2017.
[39] F. Wang, Y. Chen, and M. Liu, "Pth moment exponential stability of stochastic memristor-based bidirectional associative memory (BAM) neural networks with time delays," *Neural Netw.*, vol. 98, pp. 192–202, Feb. 2018.
[40] M. Yuan, W. Wang, X. Luo, and L. Li, "Asymptotic anti-synchronization of memristor-based BAM neural networks with probabilistic mixed time-varying delays and its application," *Mod. Phys. Lett. B*, vol. 32, no. 24, Aug. 2018, Art. no. 1850287.

[41] C. Chen, L. Li, H. Peng, and Y. Yang, "Adaptive synchronization of memristor-based BAM neural networks with mixed delays," *Appl. Math. Comput.*, vol. 322, pp. 100–110, Apr. 2018.
[42] P. Dorato, *Short-Time Stability in Linear Time-Varying Systems*. New York, NY, USA: Polytechnic Institute of Brooklyn, Microwave Research Institute, 1961.
[43] J. Xiao, S. Zhong, Y. Li, and F. Xu, "Finite-time Mittag–Leffler synchronization of fractional-order memristive BAM neural networks with time delays," *Neurocomputing*, vol. 219, pp. 431–439, Jan. 2017.
[44] L. Wang and Y. Shen, "Finite-time stabilizability and instabilizability of delayed memristive neural networks with nonlinear discontinuous controller," *IEEE Trans. Neural Netw. Learn. Syst.*, vol. 26, no. 11, pp. 2914–2924, Nov. 2015.
[45] C. Chen, L. Li, H. Peng, Y. Yang, and T. Li, "Finite-time synchronization of memristor-based neural networks with mixed delays," *Neurocomputing*, vol. 235, pp. 83–89, Apr. 2017.
[46] X. Qin, C. Wang, L. Li, H. Peng, Y. Yang, and L. Ye, "Finite-time modified projective synchronization of memristor-based neural network with multi-links and leakage delay," *Chaos, Solitons Fractals*, vol. 116, pp. 302–315, Nov. 2018.
[47] Y. Zhang, L. Li, H. Peng, J. Xiao, Y. Yang, M. Zheng, and H. Zhao, "Finite-time synchronization for memristor-based BAM neural networks with stochastic perturbations and time-varying delays," *Int. J. Robust Nonlinear Control*, vol. 28, no. 16, pp. 5118–5139, Nov. 2018.
[48] B. Qiu, L. Li, H. Peng, and Y. Yang, "Synchronization of multi-links memristor-based switching networks under uniform random attacks," *Neural Process. Lett.*, vol. 48, no. 3, pp. 1431–1458, Dec. 2018.
[49] M. S. Ali and S. Saravanan, "Finite-time stability for memristor based switched neural networks with time-varying delays via average dwell time approach," *Neurocomputing*, vol. 275, pp. 1637–1649, Jan. 2018.
[50] A. F. Filippov, *Differential Equations With Discontinuous Righthand Sides: Control Systems* (Mathematics and its Applications), vol. 18, F. Arscott, Ed. Dordrecht, The Netherlands: Springer, 2013.
[51] Y. Tang, "Terminal sliding mode control for rigid robots," *Automatica*, vol. 34, no. 1, pp. 51–56, Jan. 1998.
[52] H. K. Khalil and J. W. Grizzle, *Nonlinear Systems*, vol. 3. Upper Saddle River, NJ, USA: Prentice-Hall, 2002.
[53] F. H. Clarke, "Nonsmooth analysis and optimization," in *Proc. Int. Congr. Math.*, vol. 5. Helsinki, Finland: Citeseer, 1983, pp. 847–853.
[54] A. Abdurahman, H. Jiang, and Z. Teng, "Finite-time synchronization for memristor-based neural networks with time-varying delays," *Neural Netw.*, vol. 69, pp. 20–28, Sep. 2015.
[55] L. Wang, Y. Shen, and G. Zhang, "Finite-time stabilization and adaptive control of memristor-based delayed neural networks," *IEEE Trans. Neural Netw. Learn. Syst.*, vol. 28, no. 11, pp. 2648–2659, Nov. 2017.
[56] X. Liu, J. Lam, W. Yu, and G. Chen, "Finite-time consensus of multiagent systems with a switching protocol," *IEEE Trans. Neural Netw. Learn. Syst.*, vol. 27, no. 4, pp. 853–862, Apr. 2016.
[57] X. Liu, H. Su, and M. Z. Q. Chen, "A switching approach to designing finite-time synchronization controllers of coupled neural networks," *IEEE Trans. Neural Netw. Learn. Syst.*, vol. 27, no. 2, pp. 471–482, Feb. 2016.

SHAOFANG WANG received the B.S. degree from the School of Computer Science and Technology, Wuhan Institute of Technology, Wuhan, China, in 2009, and the M.S. degree in computer applied technology from the Wuhan University of Technology, Wuhan, in 2012. She is currently pursuing the Ph.D. degree with the Beijing University of Posts and Telecommunications, Beijing, China. Her current research interests include complex dynamical networks, memristor-based neural networks, and fractional-order systems.

LIXIANG LI received the M.S. degree in circuit and system from Yanshan University, Qinhuangdao, China, in 2003, and the Ph.D. degree in signal and information processing from the Beijing University of Posts and Telecommunications, Beijing, China, in 2006. She visited the Potsdam Institute for Climate Impact Research, Germany, in 2011. She is currently a Professor with the School of Cyberspace Security, Beijing University of Posts and Telecommunications. She is the coauthor of more than 100 articles. Her research interests include compressive sensing, swarm intelligence, and network security. She was a National Excellent Doctoral Theses winner, the New Century Excellent Talents in University, Hong Kong Scholar Award winner, and Beijing Higher Education Program for Young Talents winner.

HAIPENG PENG received the M.S. degree in system engineering from the Shenyang University of Technology, Shenyang, China, in 2006, and the Ph.D. degree in signal and information processing from the Beijing University of Posts and Telecommunications, Beijing, China, in 2010. He is currently a Professor with the School of Cyberspace Security, Beijing University of Posts and Telecommunications. He is the coauthor of 60 articles. His research interests include compressive sensing, information security, network security, and complex networks.

YIXIAN YANG received the M.S. degree in applied mathematics and the Ph.D. degree in electronics and communication systems from the Beijing University of Posts and Telecommunications, Beijing, China, in 1986 and 1988, respectively. He is currently the Managing Director of the Information Security Center, Beijing University of Posts and Telecommunications. He is the Yangtze River Scholar Program Professor. He has authored more than 40 national and provincial key scientific research projects. He has published more than 300 high-level articles and 20 monographs. His major research interests include coding and cryptography, information and network security, and signal and information processing. He is the National Outstanding Youth Fund winners and the National Teaching Masters.

MINGWEN ZHENG received the B.S. degree from the School of Science, Shan Dong University of Technology, Zibo, China, in 2002, and the M.S. degree from the School of Computer and Communication Engineering, China University of Petroleum, Dong Ying, China, in 2009. He is currently an Associate Professor with the Shandong University of Technology. His current research interests include complex dynamical networks, memristor-based neural networks, and fractional-order systems.